Supplementary Materials

Results of Sequential Models

Sequential models feature two boundary queries between phases, which allow for time lapses to have occurred between them. As expected, these sequential models (denominated with an "S") show the Texoloc phase starting at a 'younger' date, generally 30-50 years younger than the results of contiguous modeling (Table S1 and Figure S1). In these variant models, the mode is now located between 600 and 550 cal BC (Model 6S is an exception given its mode around 650 cal BC). The agreement indices were consistently lower across the sequential models compared to their contiguous counterparts (this was not the case for Model 2 and 2S). Given that the same set of samples was used to construct the contiguous and sequential iterations, this decrease indicates a poorer fit with the data. Although there were no substantial differences regarding the end date of the Texoloc phase between the contiguous and sequential modeling (Table S2), we think contiguous models account for our data better and, therefore, constitute more valid models.

Table S1. Date ranges for the Tlatempa-Texoloc boundaries (more likely 1σ and 2σ date ranges are in bold).

	1 σ cal BC	P	Mode*	2 σ cal BC	P	Mode*	Mean	Median
Phase method								
Model 1S (all samples)	681-642 BC	26.3%	650 (670) BC	**706-553 BC**	95.4%	585 (650) BC	624 BC	618 BC
	605-556 BC	41.9%	585 (570) BC					
Model 2S (Complex C)	**680-610 BC**	50.2%	650 BC	**708-559 BC**	95.4%	650 (590) BC	634 BC	635 BC
	605-580 BC	18.0%	590 BC					
Model 3S (Complex TM)	681-640 BC	28.0%	650 BC	**708-553 BC**	95.4%	585 (650) BC	626 BC	623 BC
	607-557 BC	40.3%	585 BC					
Phase/Sequence method								
Model 6S (Complex C)	**700-634 BC**	53.1%	655 BC	**717-612 BC**	73.1%	655 BC	642 BC	652 BC
	626-619 BC	3.2%	620 BC	602-556 BC	22.3%	585 BC		
	596-575 BC	11.9%	585 BC					
Model 7S (Complex TM)	**636-552 BC**	68.3%	590 BC	**698-547 BC**	95.4%	590 BC	610 BC	600 BC
Overlapping Sequence method								
Model 8S (both complexes)	669-666 BC	1.4%	—	**699-550 BC**	95.4%	565 (650) BC	611 BC	598 BC
	658-646 BC	6.5%	650 BC					
	616-553 BC	60.4%	565 BC					
Cross Referencing method								
Model 9S (both complexes)	692-691 BC	0.9%	—	706-685 BC	8.0%	—	609 BC	590 BC
	668-665 BC	1.7%	—	677-635 BC	30.2%	650 BC		
	654-642 BC	18.9%	650 BC	624-613 BC	2.3%	—		
	591-553 BC	46.8%	560 BC	**607-548 BC**	55.0%	560 BC		

* The date within parenthesis shows the secondary mode when present.

Table S2. Date ranges for the Texoloc-Tezoquipan boundaries (more likely 1σ and 2σ date ranges are in bold).

	1 σ cal BC	P	Mode*	2 σ cal BC	P	Mode*	Mean	Median
Phase method								
Model 1S (all samples)	**577-518 BC**	68.3%	545 BC	**646-502 BC**	95.4%	545 BC	563 BC	552BC
Model 2S (Complex C)	616-610 BC	2.7%	610 BC	**664-456 BC**	95.4%	545 BC	554 BC	551 BC
	588-506 BC	65.6%	545 BC					
Model 3S (Complex TM)	**581-515 BC**	68.3%	545 BC	663-657 BC	0.6%	—	562 BC	552 BC
				650-487 BC	94.9%	545 BC		
Phase/Sequence method								
Model 6S (Complex C)	**616-542 BC**	68.3%	550 BC	685-674 BC	1.3%	—	580 BC	576 BC
				645-510 BC	94.1%	550 BC		
Model 7S (Complex TM)	**551-486 BC**	68.3%	540 BC	662-640 BC	1.9%	—		
				576-409 BC	93.6%	540 BC	518 BC	524 BC
Overlapping Sequence method								
Model 8S (both complexes)	**566-493 BC**	68.3%	545 BC	687-684 BC	0.2%	—	535 BC	537 BC
				648-424 BC	95.2%	545 BC		
Cross Referencing method								
Model 9S (both complexes)	693-688 BC	2.4%	—	699-602 BC	36.6%	645 BC	586 BC	568 BC
	651-634 BC	19.2%	645 BC	**594-483 BC**	58.9%	560 BC		
	588-535 BC	46.6%	560 BC					

* The date within parenthesis shows the secondary mode when present.

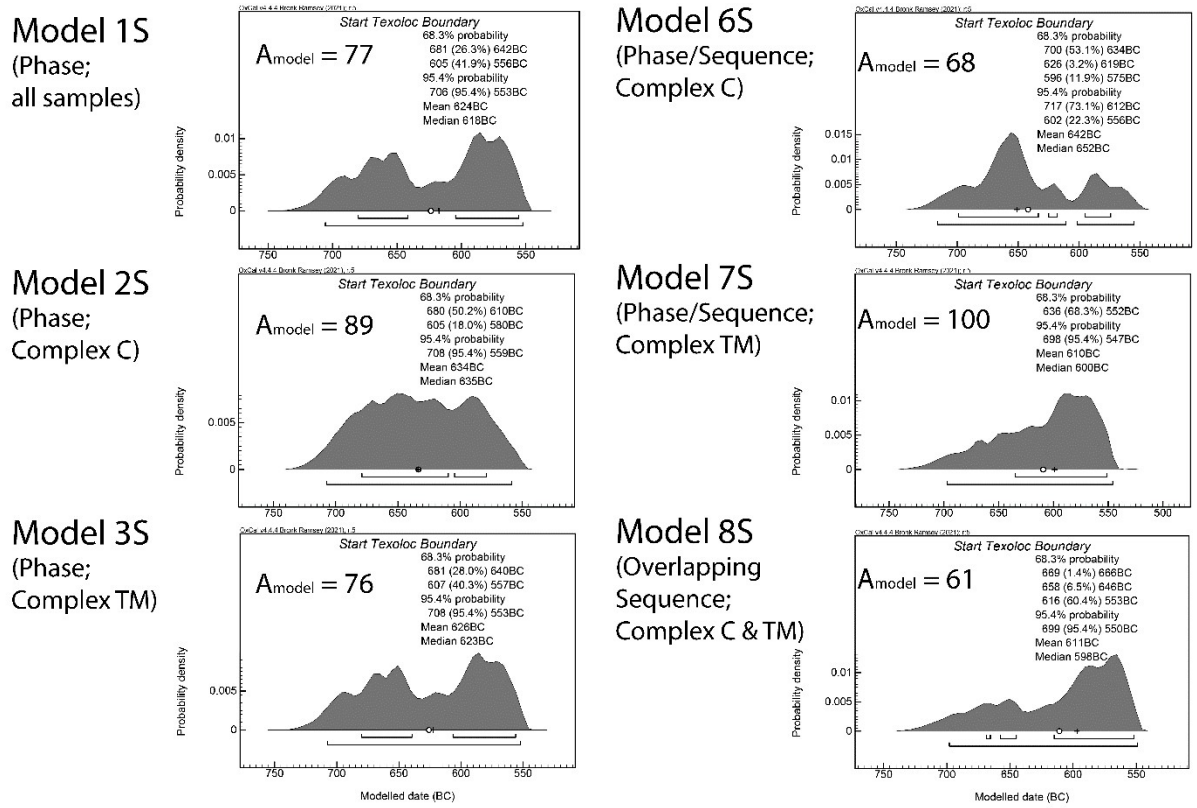

Figure S1. Tlatempa-Texoloc boundaries for sequential models. Horizontal bars under the distributions are at 1σ and 2σ probability ranges.

Figures

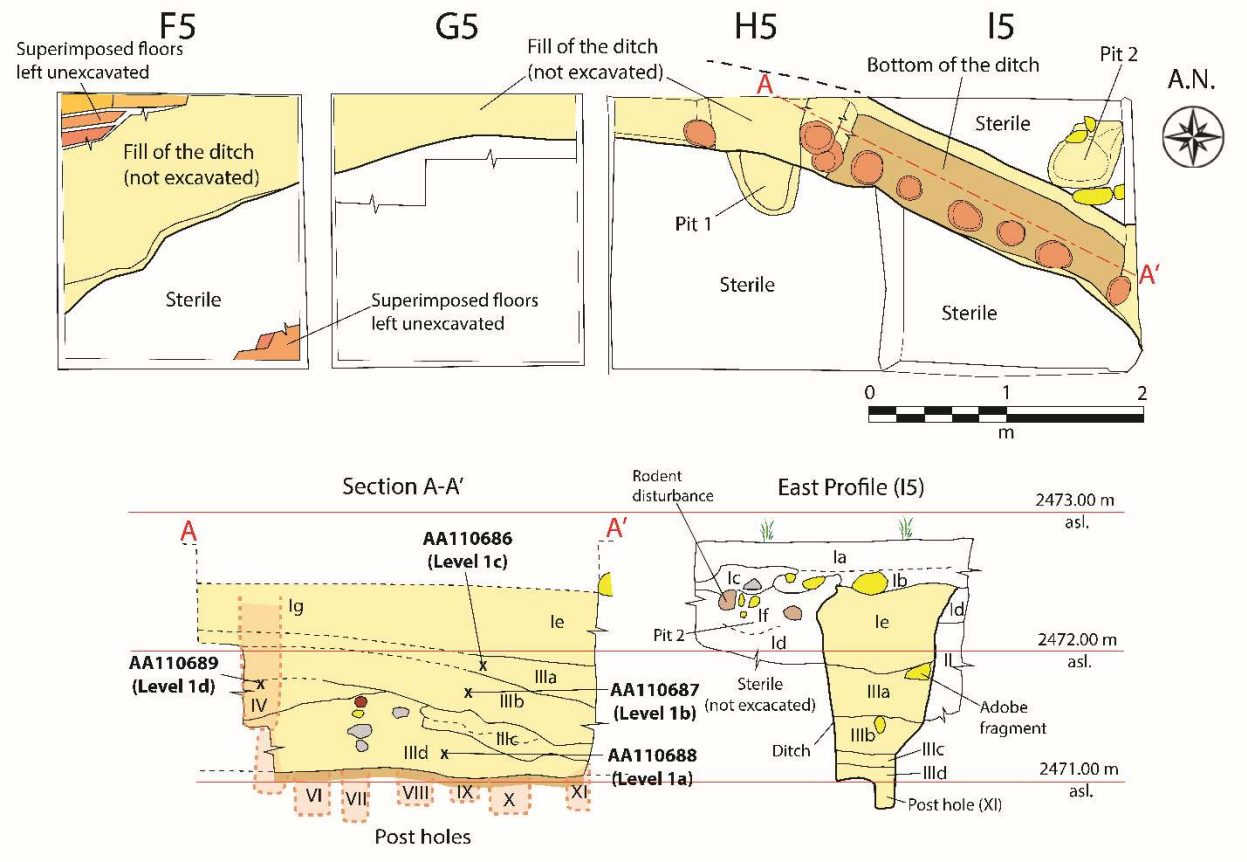

Figure S2. Stratigraphy of the ditched palisade showing the provenience of four radiocarbon samples (AA-110686－110689) from the ditched palisade at Complex C (see Figure 3 for the location of the ditched palisade).

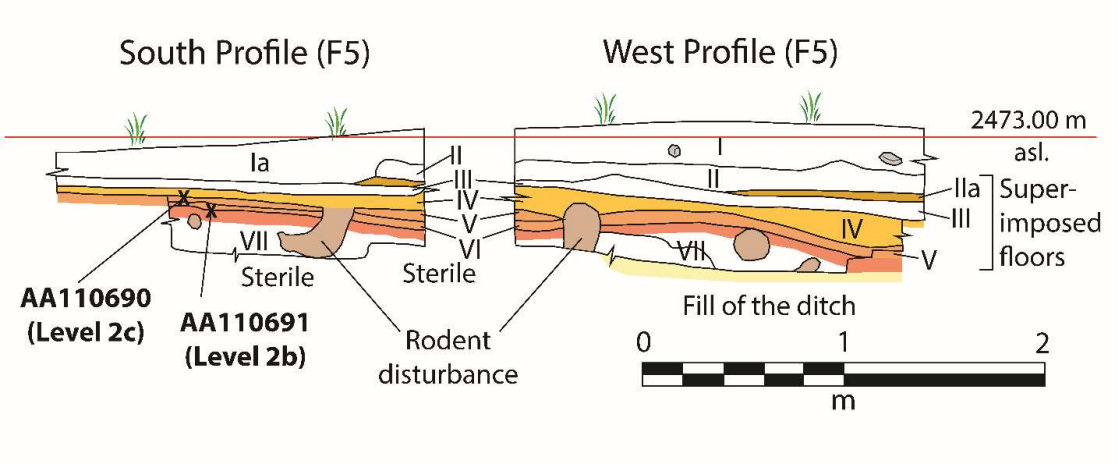

Figure S3. Stratigraphy of the section F5 showing the provenience of two radiocarbon samples (AA-110690 and AA-110691) at Complex C (see Figures 3 and S1 for the location of F5).

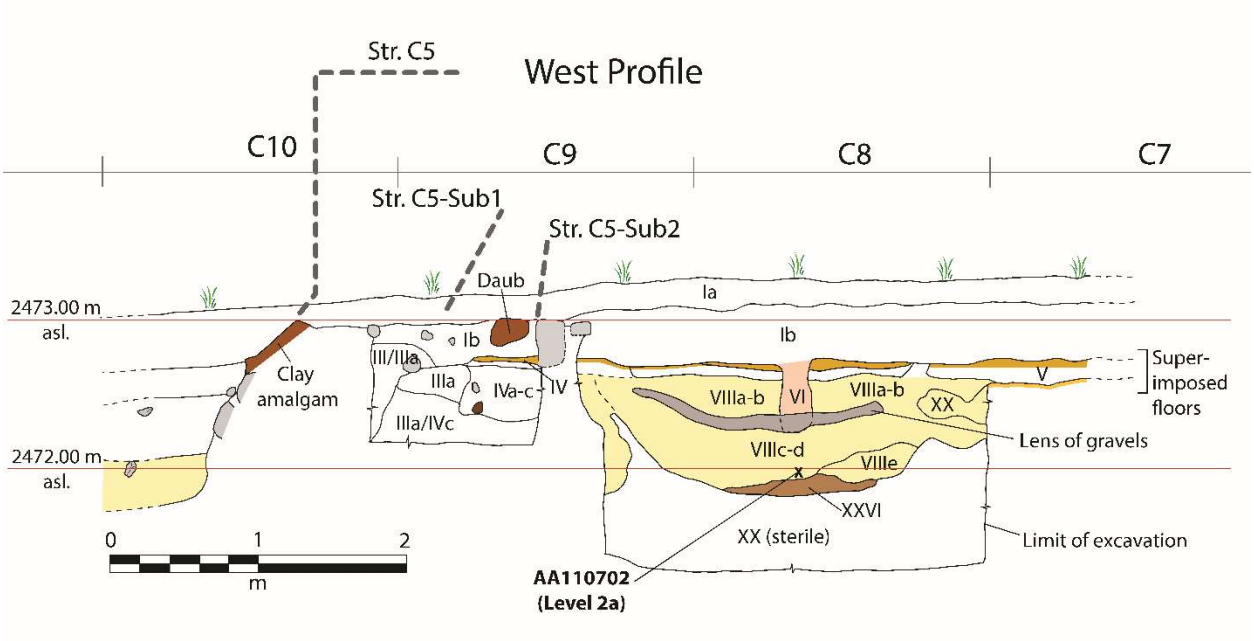

Figure S4. Stratigraphy of the sections C7 to C10 showing the provenience of one radiocarbon sample (AA-110702) at Complex C (see Figures 3 for the location of these sections).

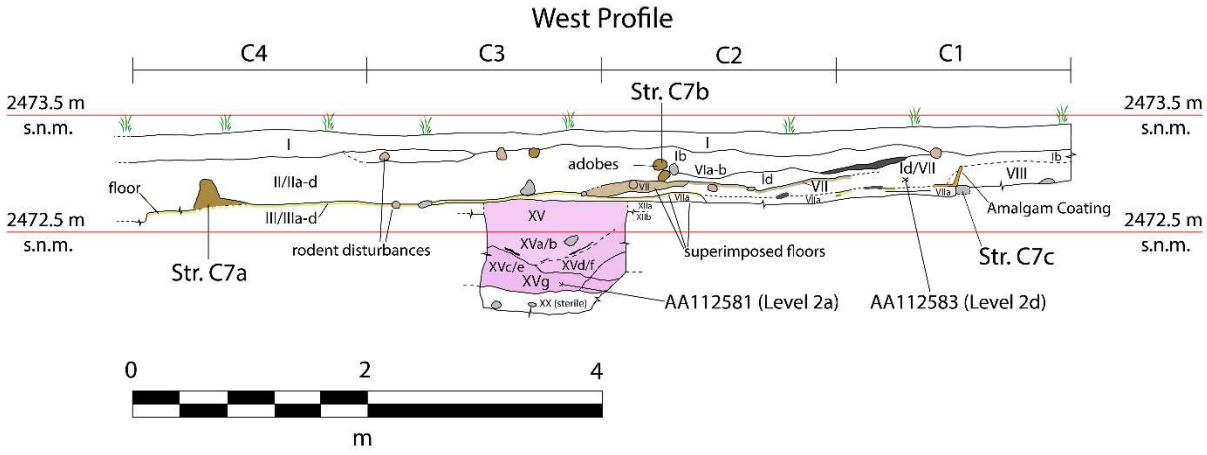

Figure S5. Stratigraphy of the sections C1 to C4 showing the provenience of two radiocarbon samples (AA-112581 and AA-112583) at Complex C (see Figures 3 for the location of these sections).

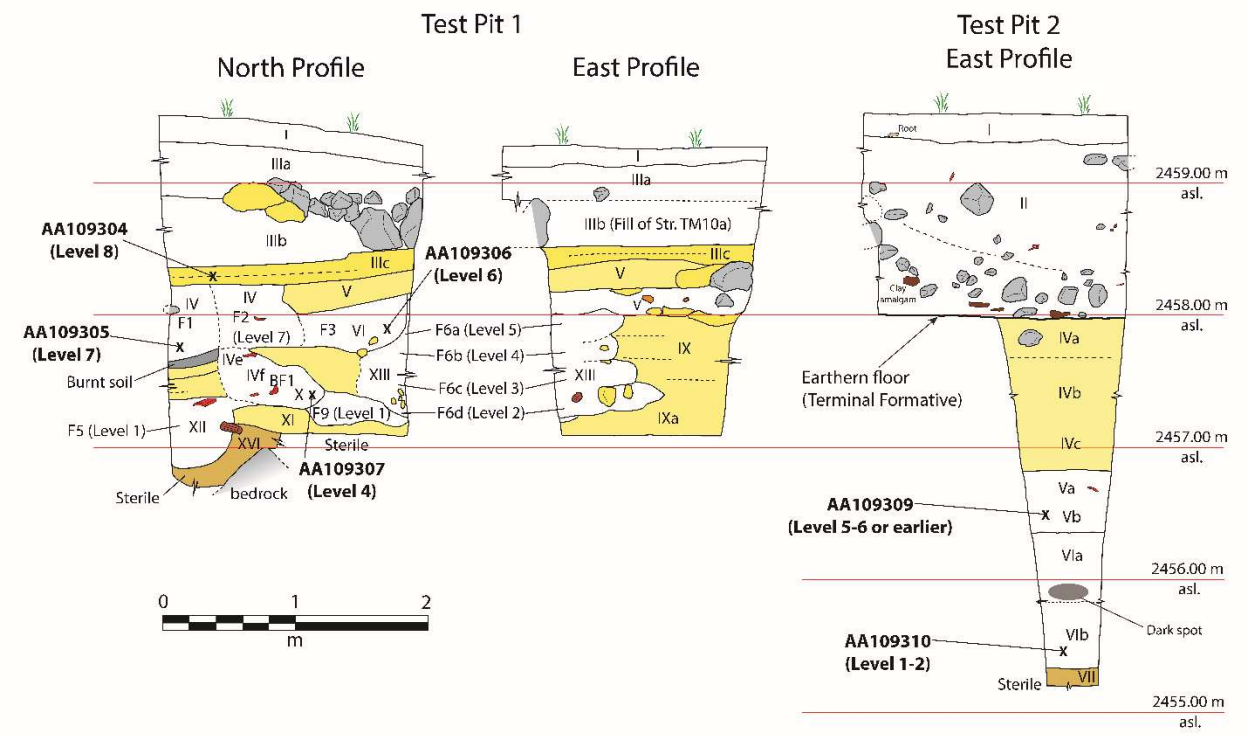

Figure S6. Stratigraphy of Test Pits 1 and 2 showing the provenience of six radiocarbon samples (AA-109304 – 109307 and AA-109309 and AA-109310) at Tres Marias Complex (see Figure 4 for the location of Test Pits 1 and 2).

Figure S7. Report of Charcoal Outlier Model 1.

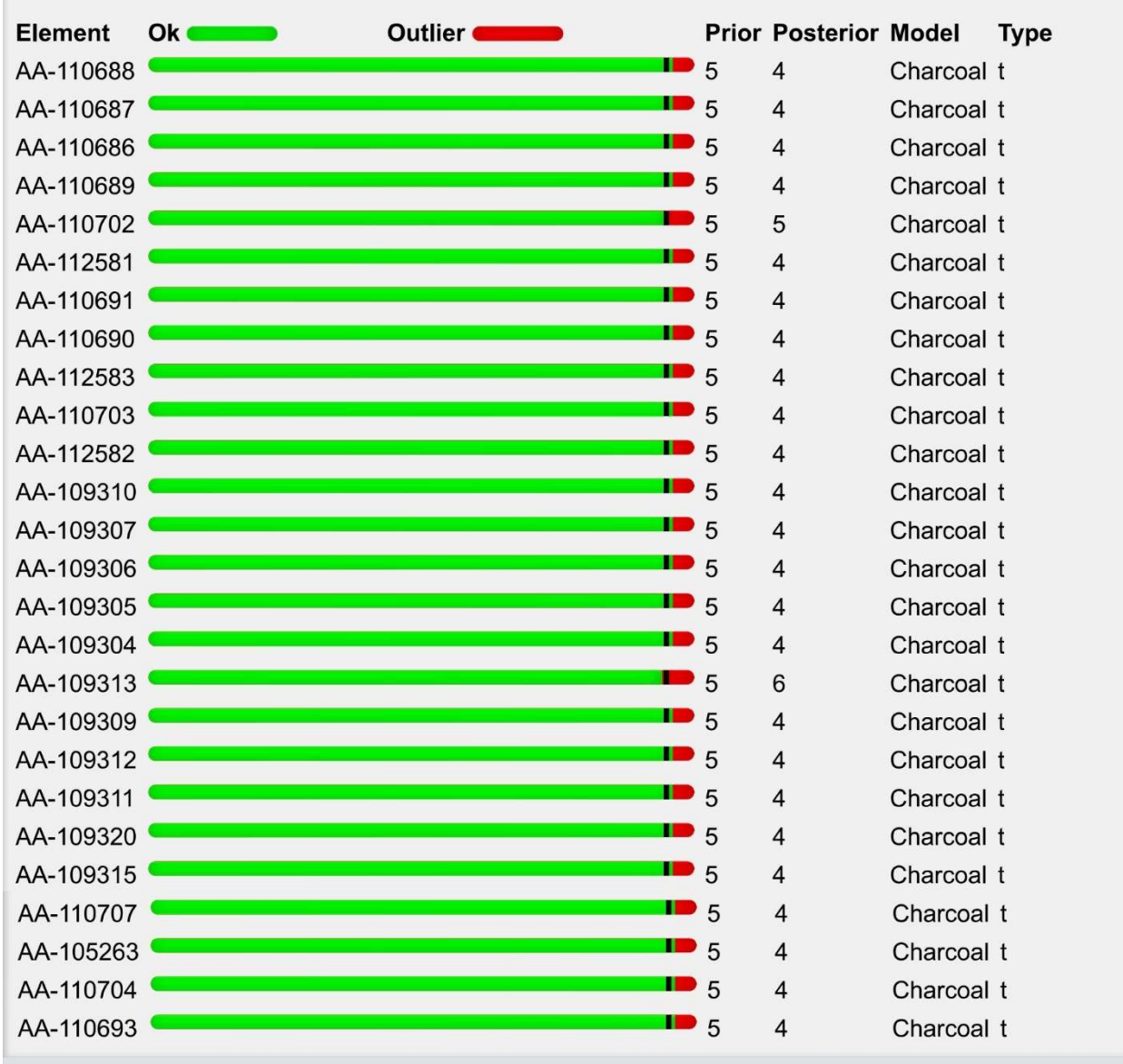

Element	Ok	Outlier	Prior	Posterior	Model	Type
AA-110688			5	4	Charcoal	t
AA-110687			5	4	Charcoal	t
AA-110686			5	4	Charcoal	t
AA-110689			5	4	Charcoal	t
AA-110702			5	5	Charcoal	t
AA-112581			5	4	Charcoal	t
AA-110691			5	4	Charcoal	t
AA-110690			5	4	Charcoal	t
AA-112583			5	4	Charcoal	t
AA-110703			5	4	Charcoal	t
AA-112582			5	4	Charcoal	t
AA-109310			5	4	Charcoal	t
AA-109307			5	4	Charcoal	t
AA-109306			5	4	Charcoal	t
AA-109305			5	4	Charcoal	t
AA-109304			5	4	Charcoal	t
AA-109313			5	6	Charcoal	t
AA-109309			5	4	Charcoal	t
AA-109312			5	4	Charcoal	t
AA-109311			5	4	Charcoal	t
AA-109320			5	4	Charcoal	t
AA-109315			5	4	Charcoal	t
AA-110707			5	4	Charcoal	t
AA-105263			5	4	Charcoal	t
AA-110704			5	4	Charcoal	t
AA-110693			5	4	Charcoal	t

Figure S8. Report of Charcoal Outlier Model 2.

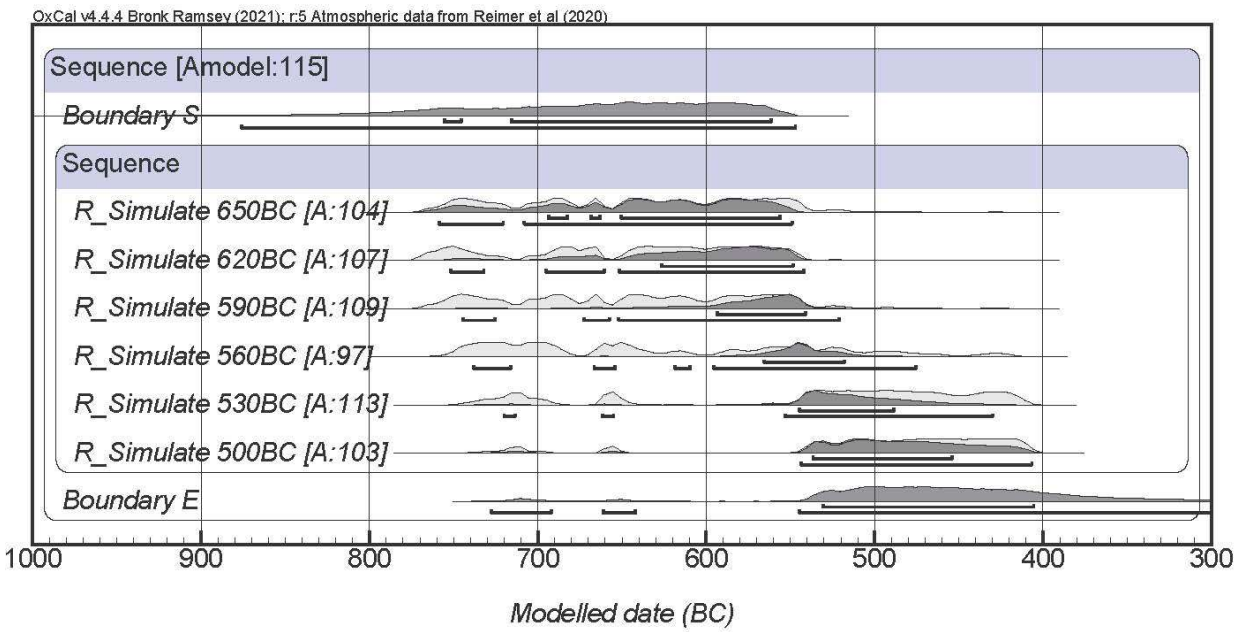

Figure S9. Simulation model based on Sequence method with 30-year intervals (6 dates) for the Texoloc phase. Horizontal bars under the distributions are at 1σ and 2σ probability ranges.

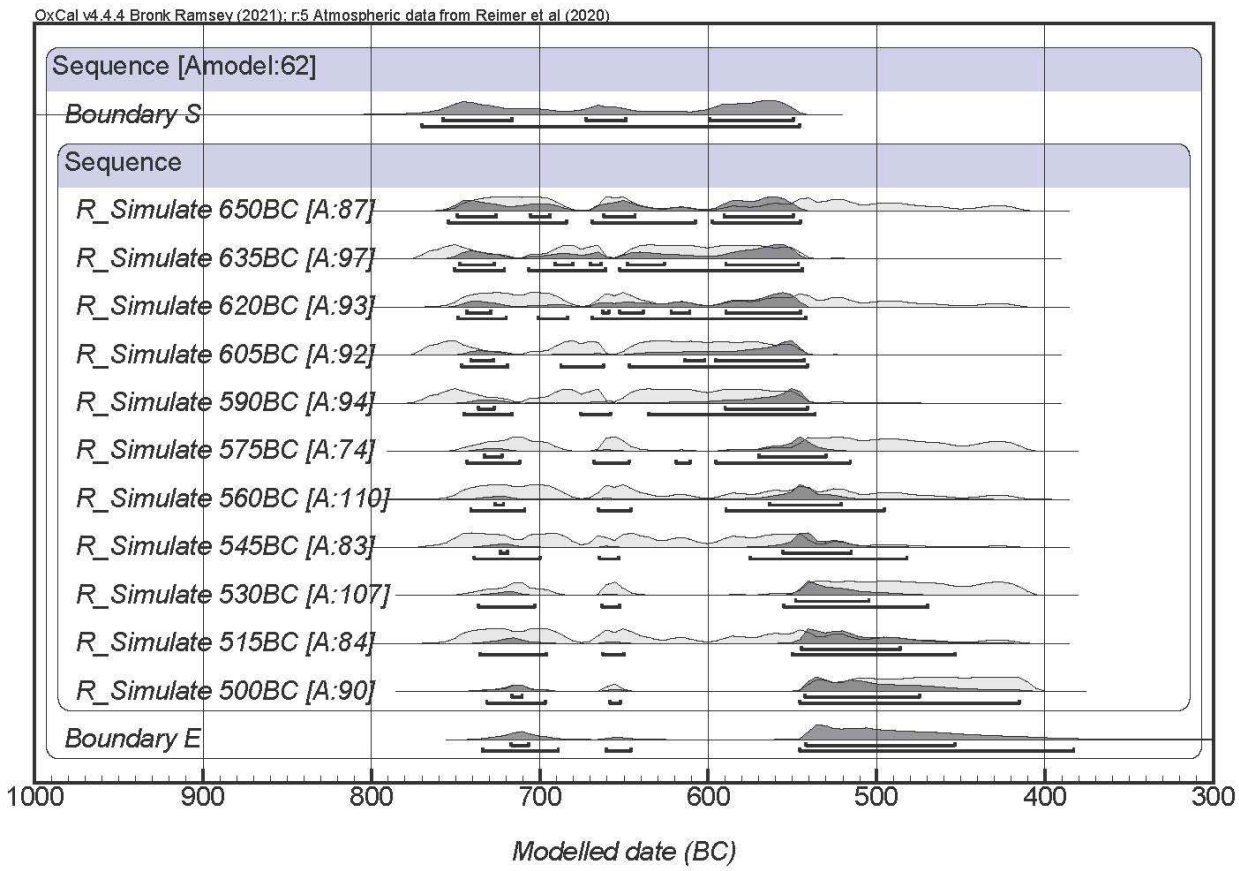

Figure S10. Simulation model based on Sequence method with 15-year intervals (11 dates) for the Texoloc phase. Horizontal bars under the distributions are at 1σ and 2σ probability ranges.

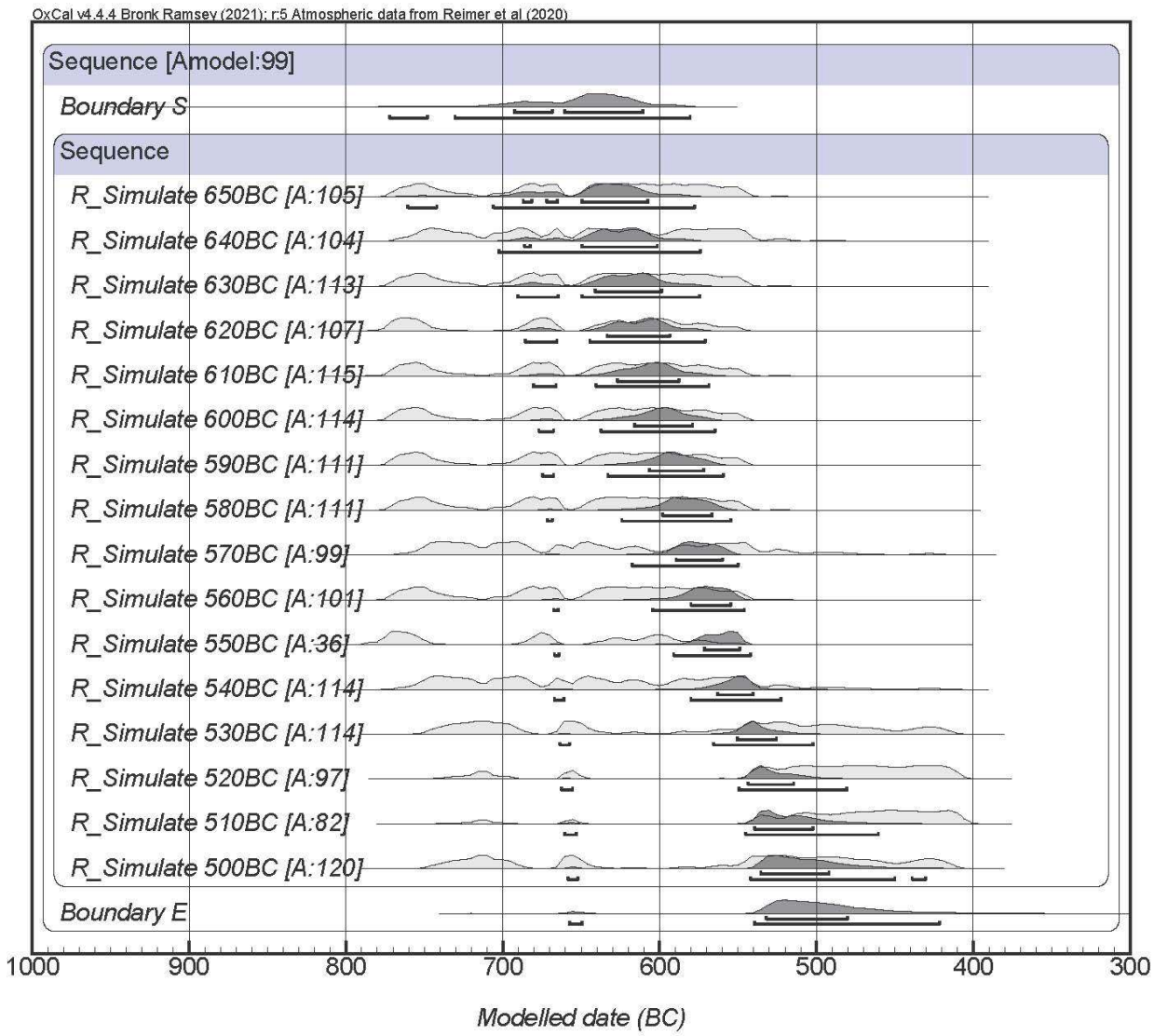

Figure S11. Simulation model based on Sequence method with 10-year intervals (16 dates) for the Texoloc phase. Horizontal bars under the distributions are at 1σ and 2σ probability ranges.

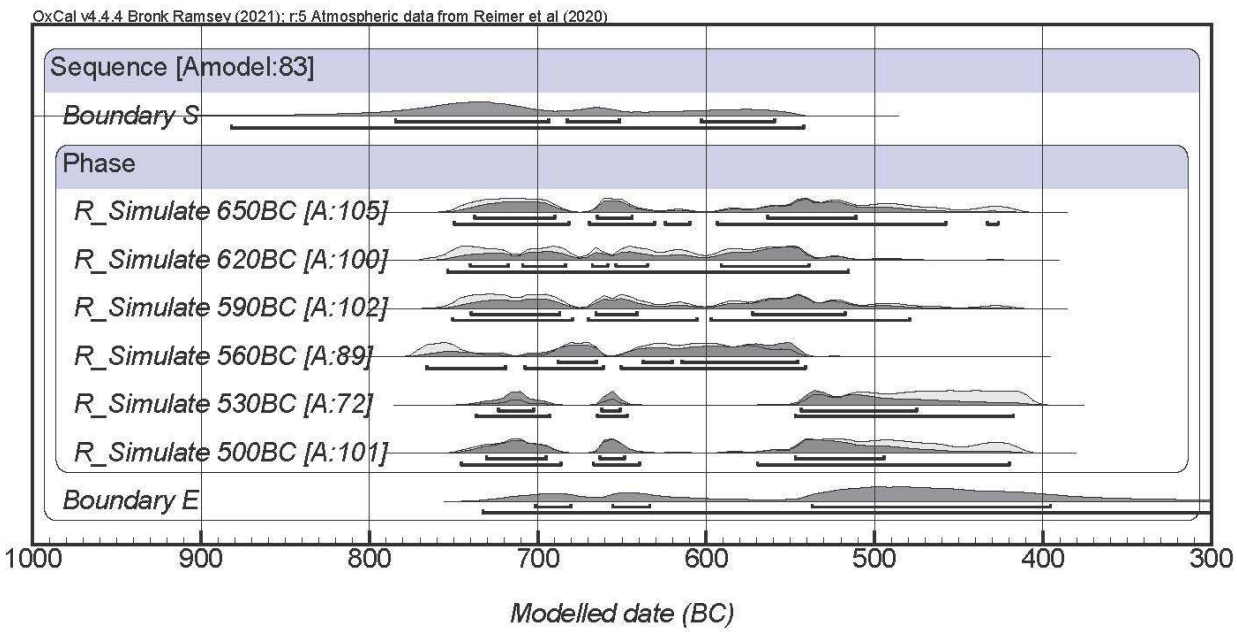

Figure S12. Simulation model based on Phase method with 30-year intervals (6 dates) for the Texoloc phase. Horizontal bars under the distributions are at 1σ and 2σ probability ranges.

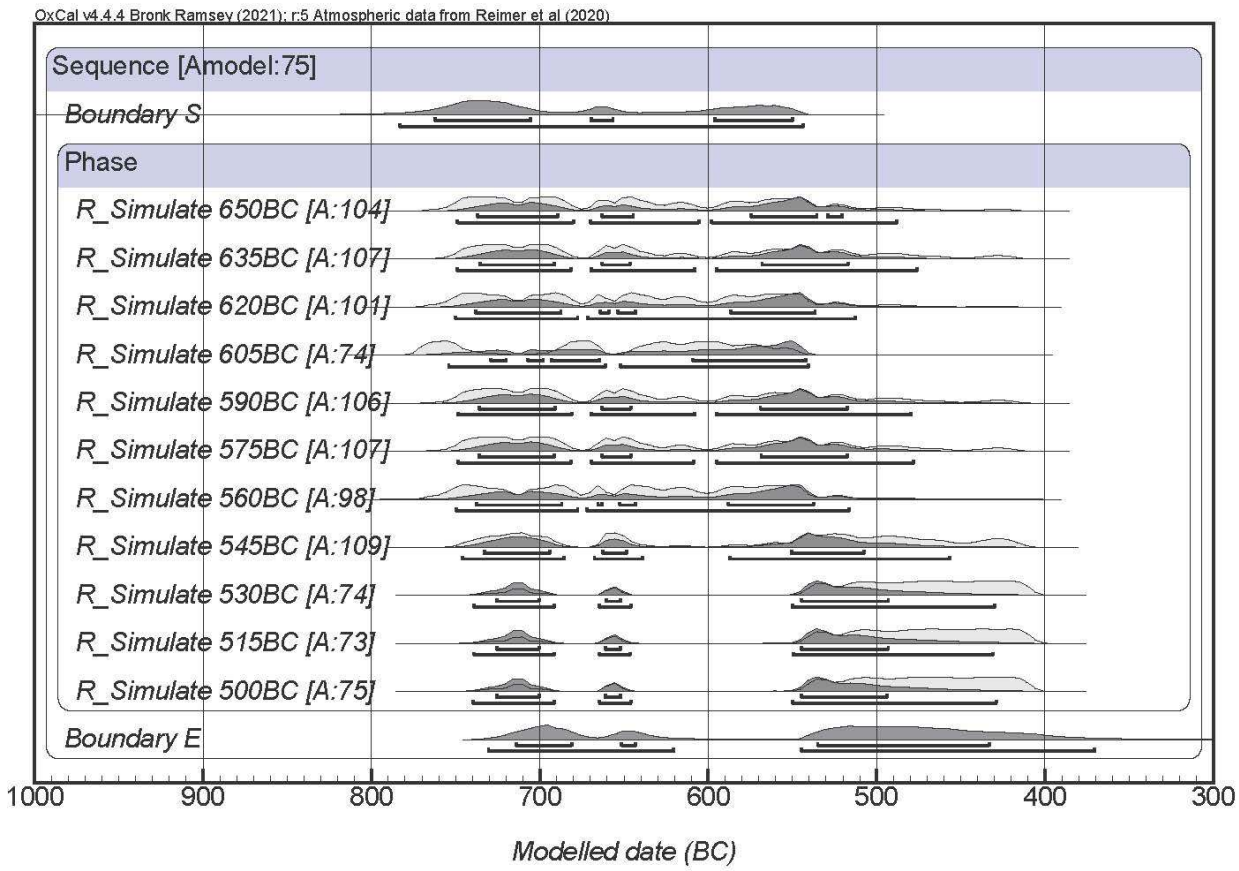

Figure S13. Simulation model based on Phase method with 15-year intervals (11 dates) for the Texoloc phase. Horizontal bars under the distributions are at 1σ and 2σ probability ranges.

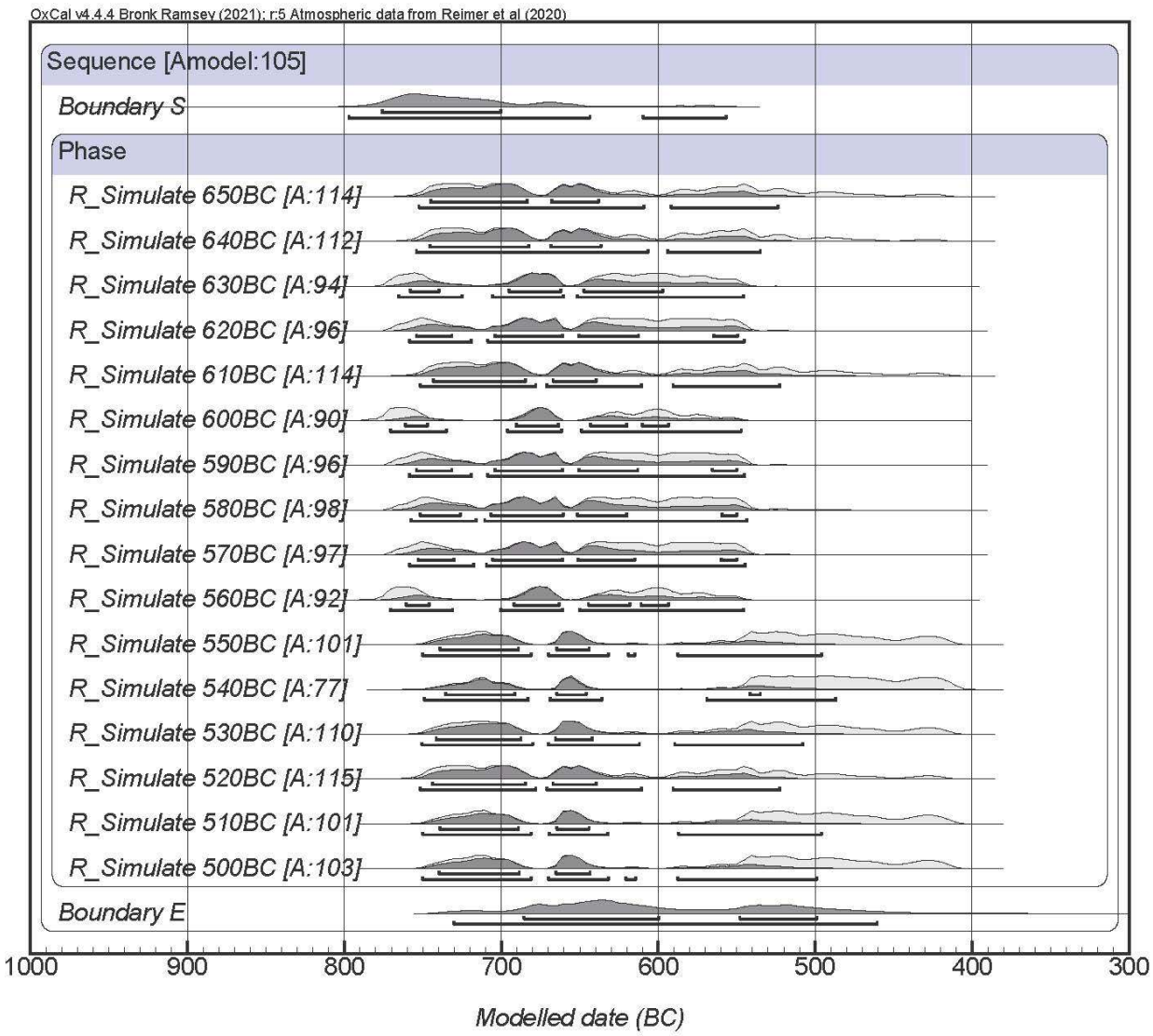

Figure S14. Simulation model based on Phase method with 10-year intervals (16 dates) for the Texoloc phase. Horizontal bars under the distributions are at 1σ and 2σ probability ranges.

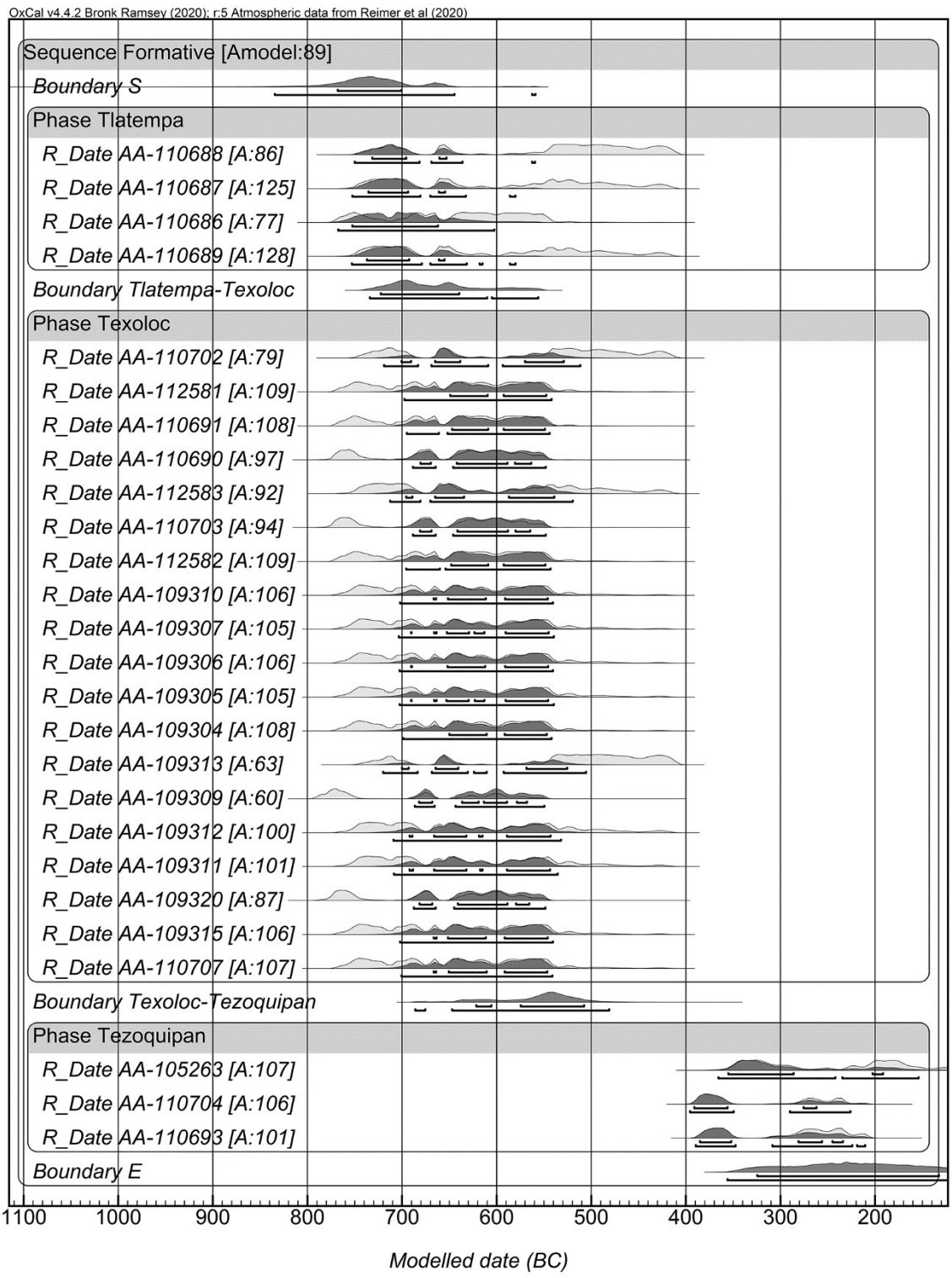

Figure S15. Bayesian Model 1 of the Middle Formative period at Tlalancaleca. Horizontal bars under the distributions are at 1σ and 2σ probability ranges.

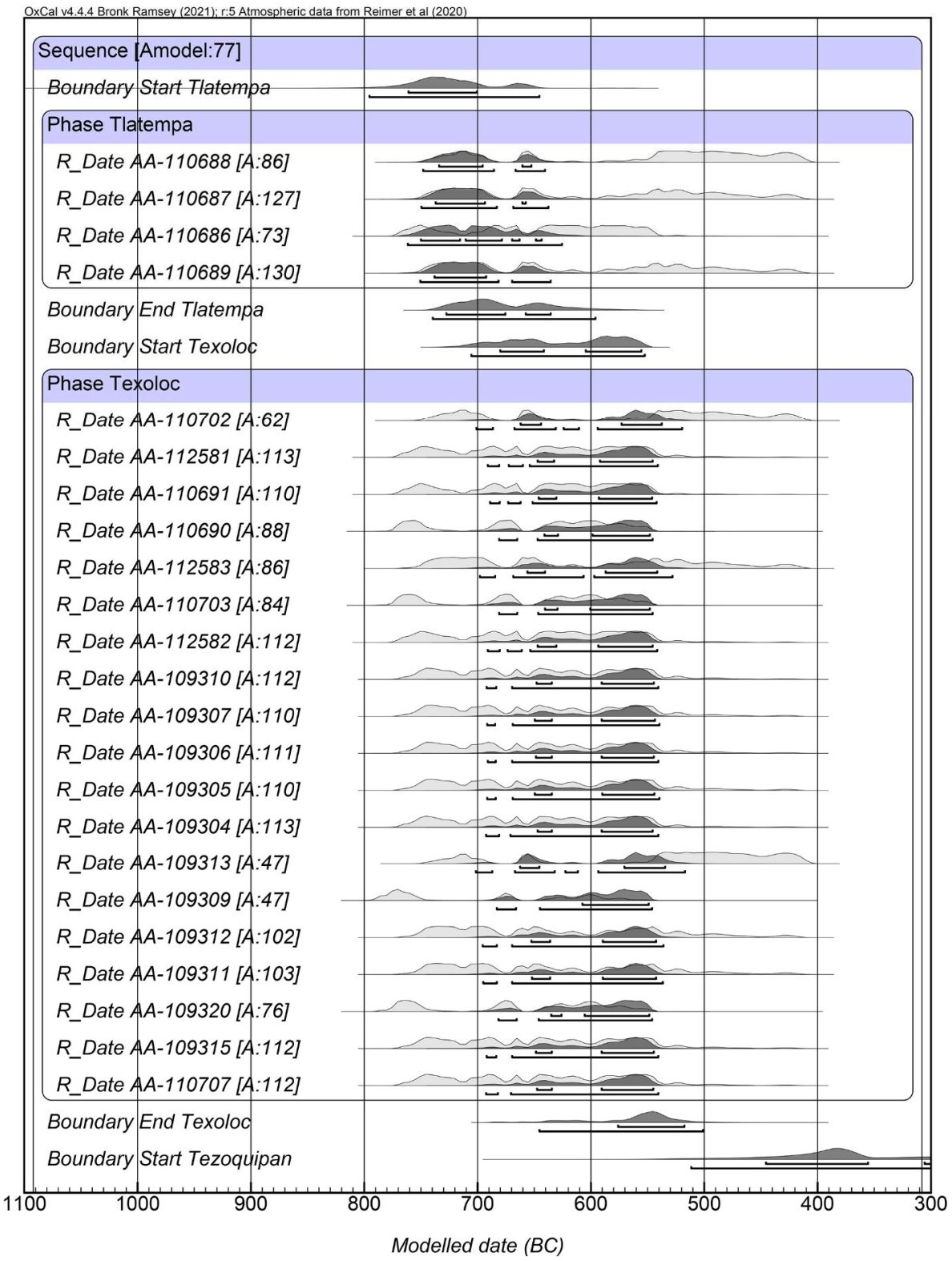

Figure S16. Bayesian Model 1S of the Middle Formative period at Tlalancaleca. Horizontal bars under the distributions are at 1σ and 2σ probability ranges.

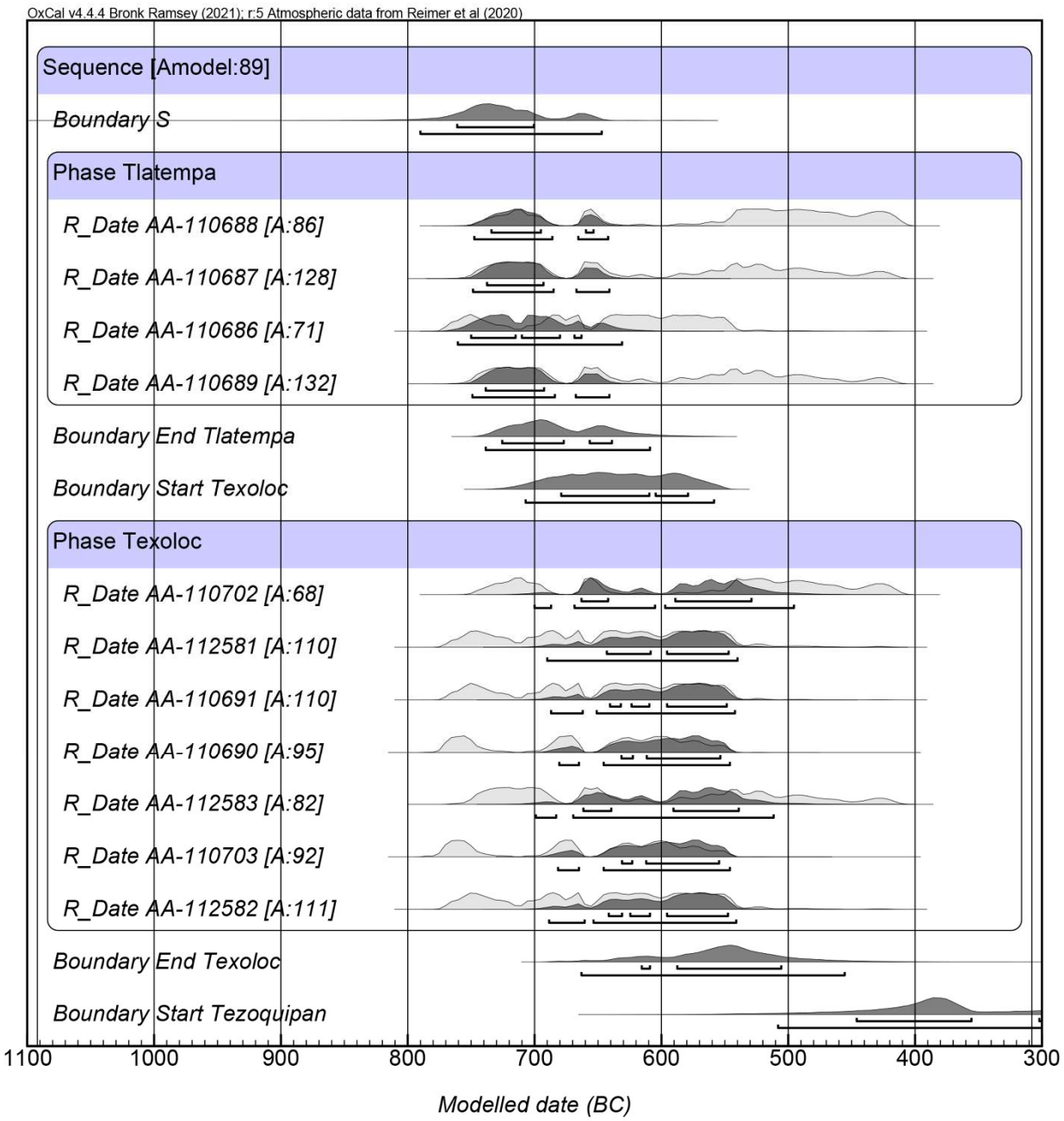

Figure S17. Bayesian Model 2 of the Middle Formative period at Tlalancaleca (Tezoquipan phase is not shown). Horizontal bars under the distributions are at 1σ and 2σ probability ranges.

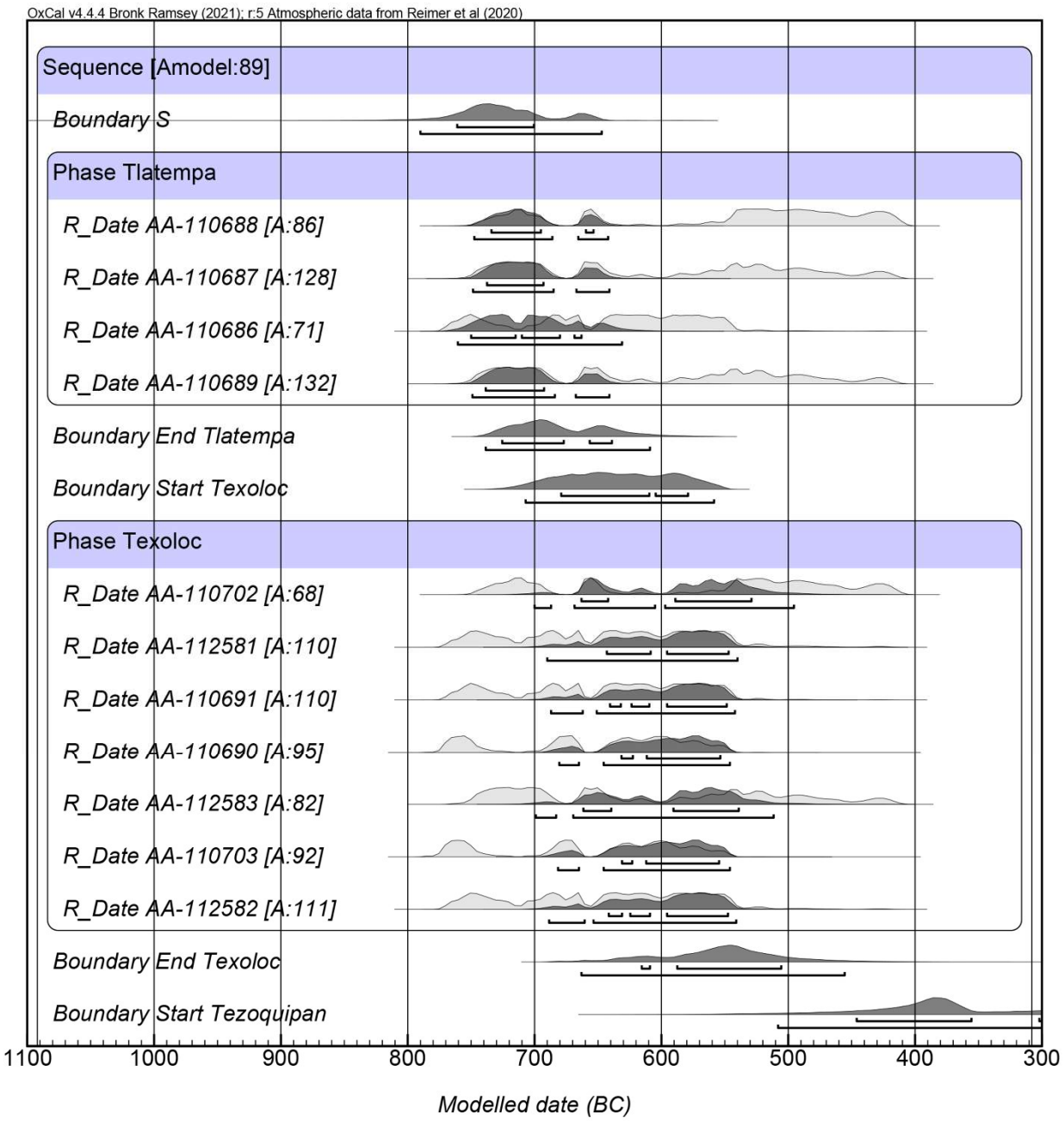

Figure S18. Bayesian Model 2S of the Middle Formative period at Tlalancaleca (Tezoquipan phase is not shown). Horizontal bars under the distributions are at 1σ and 2σ probability ranges.

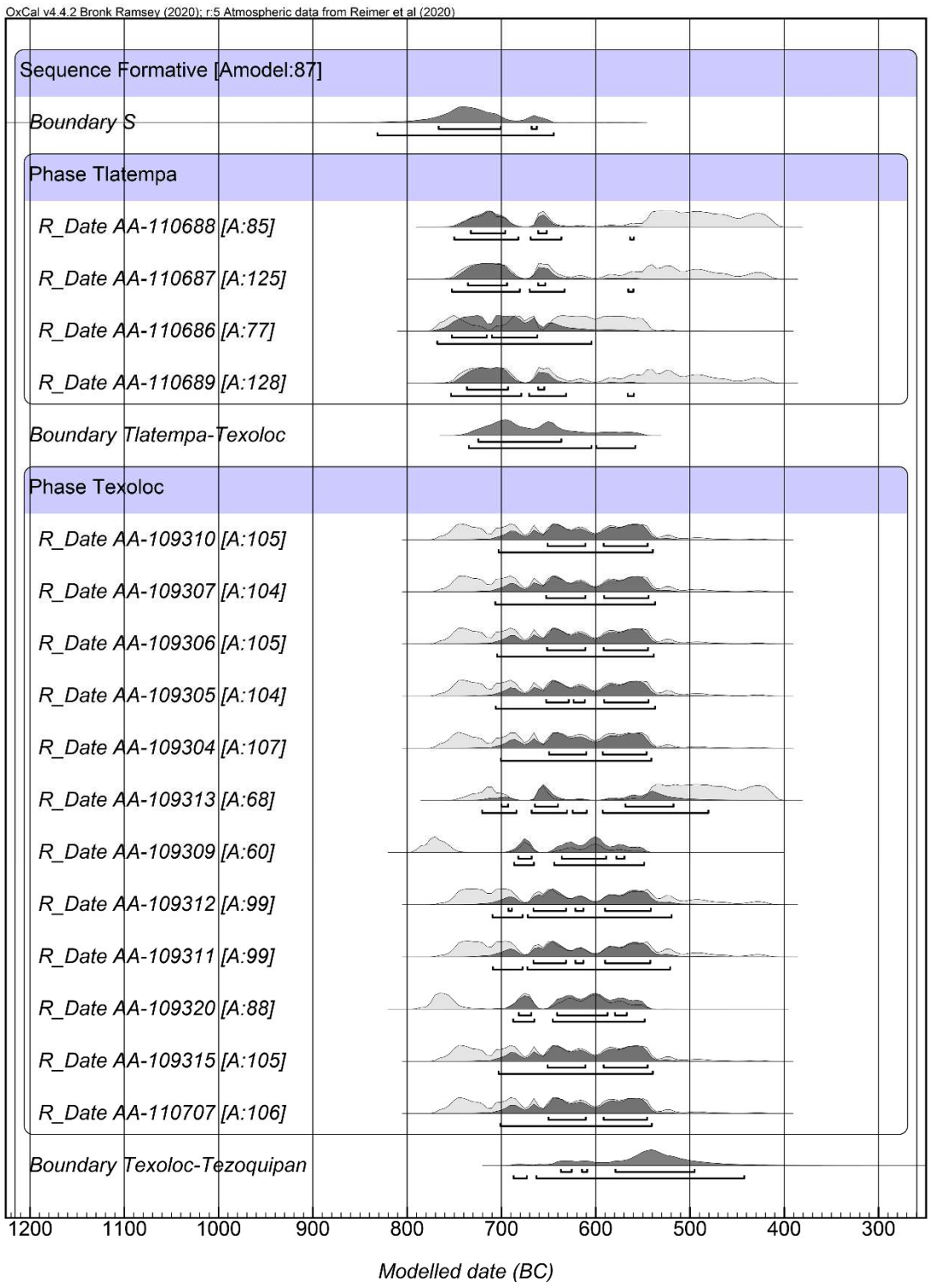

Figure S19. Bayesian Model 3 of the Middle Formative period at Tlalancaleca (Tezoquipan phase is not shown). Horizontal bars under the distributions are at 1σ and 2σ probability ranges.

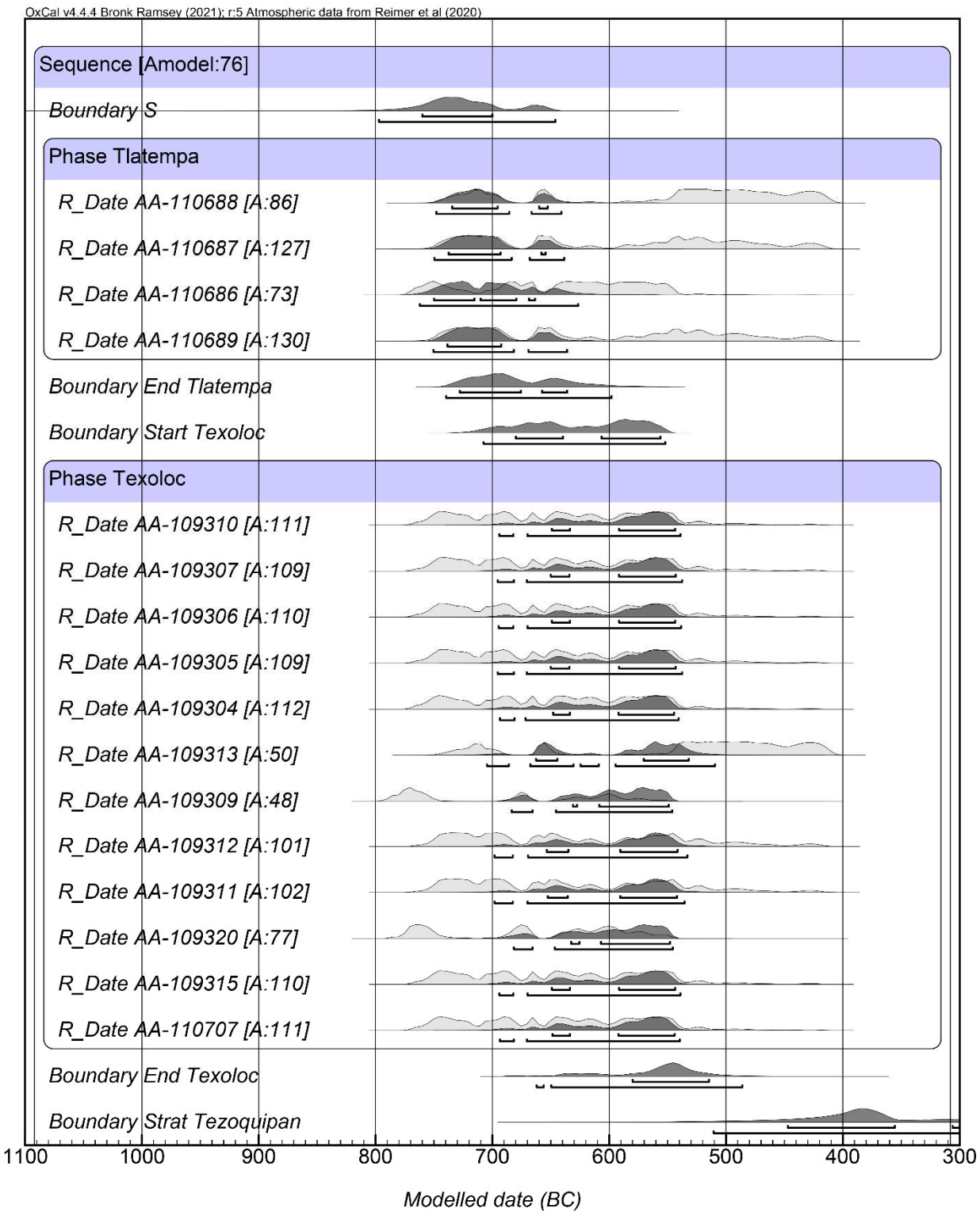

Figure S20. Bayesian Model 3S of the Middle Formative period at Tlalancaleca (Tezoquipan phase is not shown). Horizontal bars under the distributions are at 1σ and 2σ probability ranges.

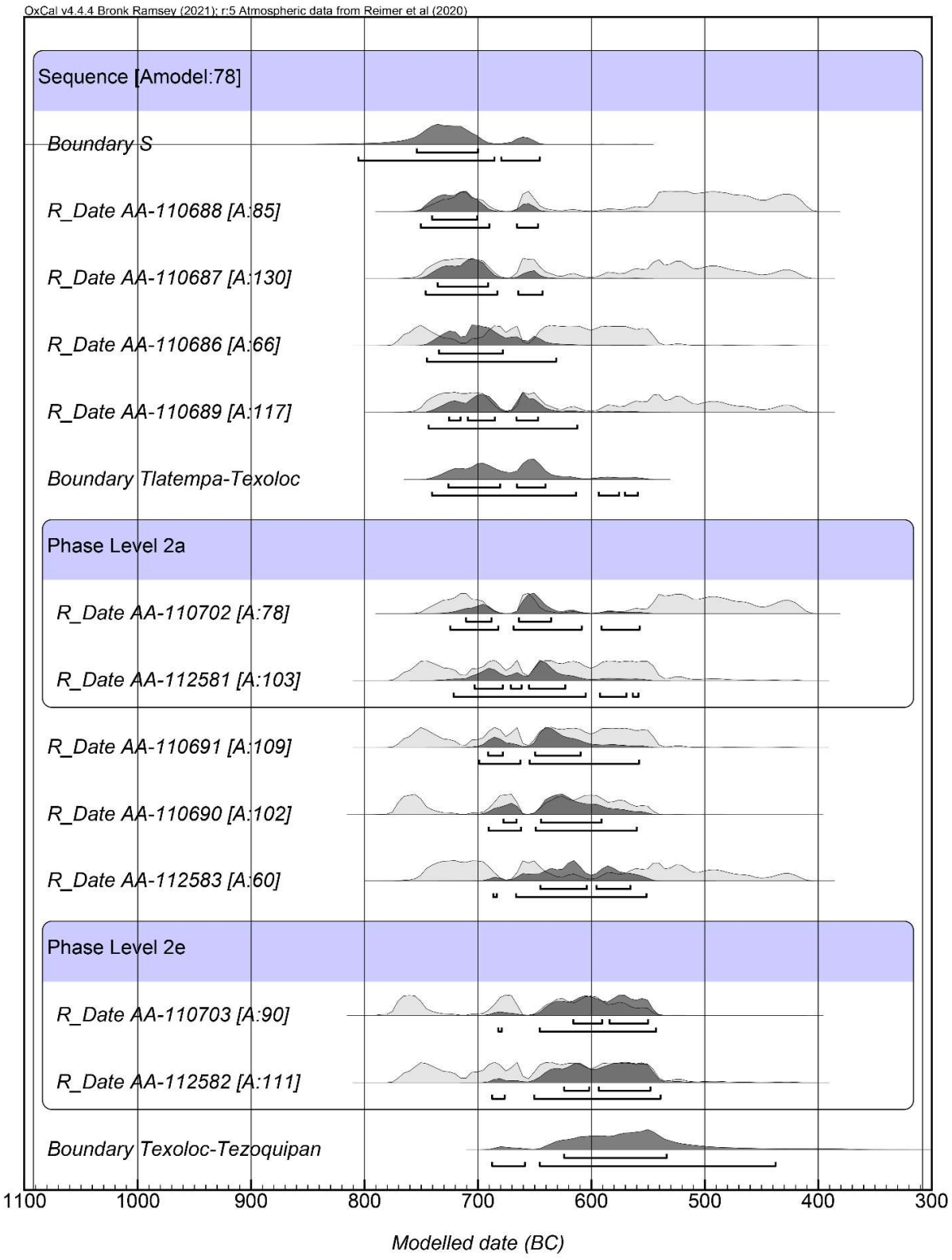

Figure S21. Bayesian Model 4 of the Middle Formative period at Tlalancaleca (Tezoquipan phase is not shown). Horizontal bars under the distributions are at 1σ and 2σ probability ranges.

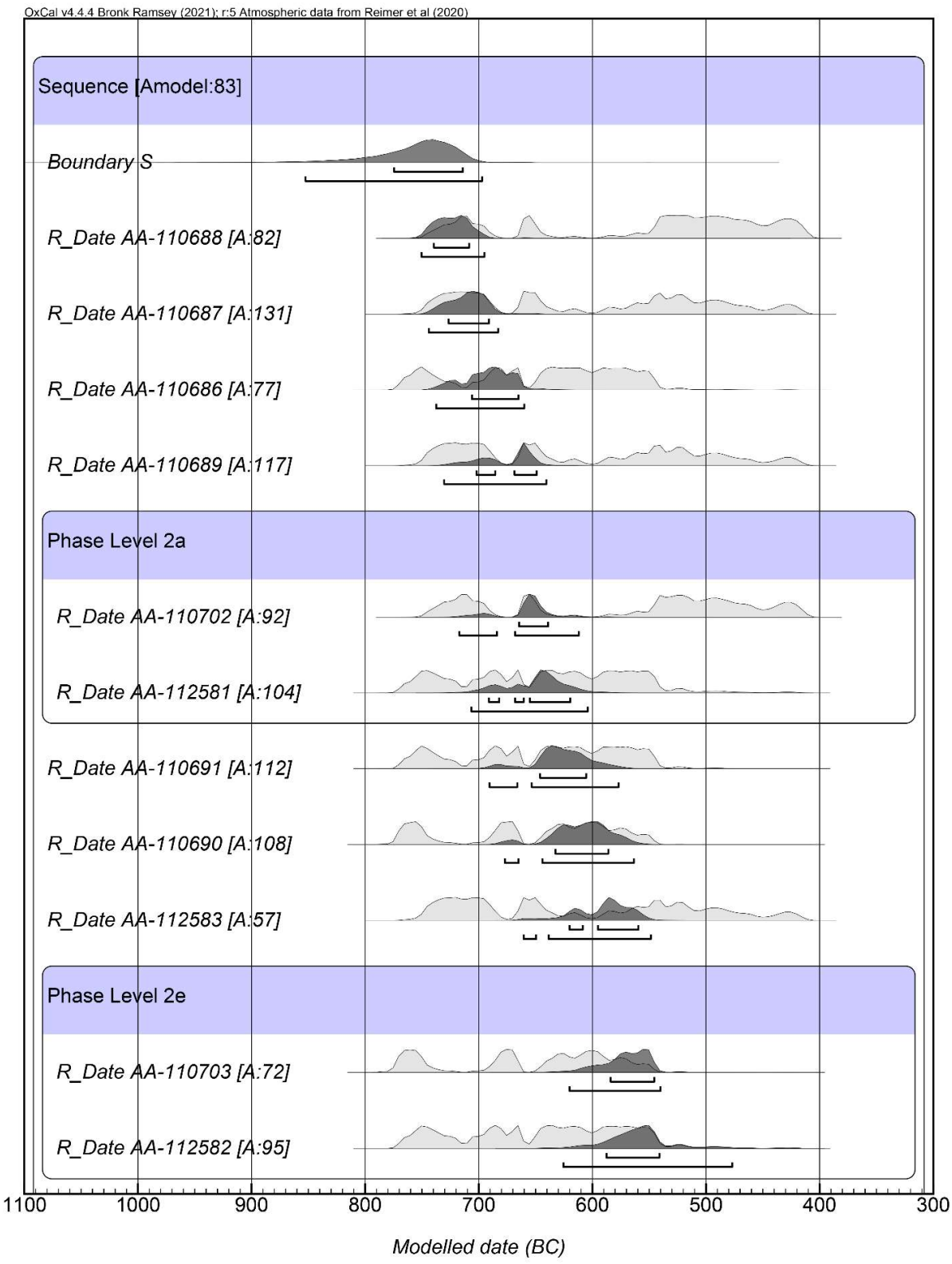

Figure S22. Bayesian Model 4NB of the Middle Formative period at Tlalancaleca (Tezoquipan phase is not shown). Horizontal bars under the distributions are at 1σ and 2σ probability ranges.

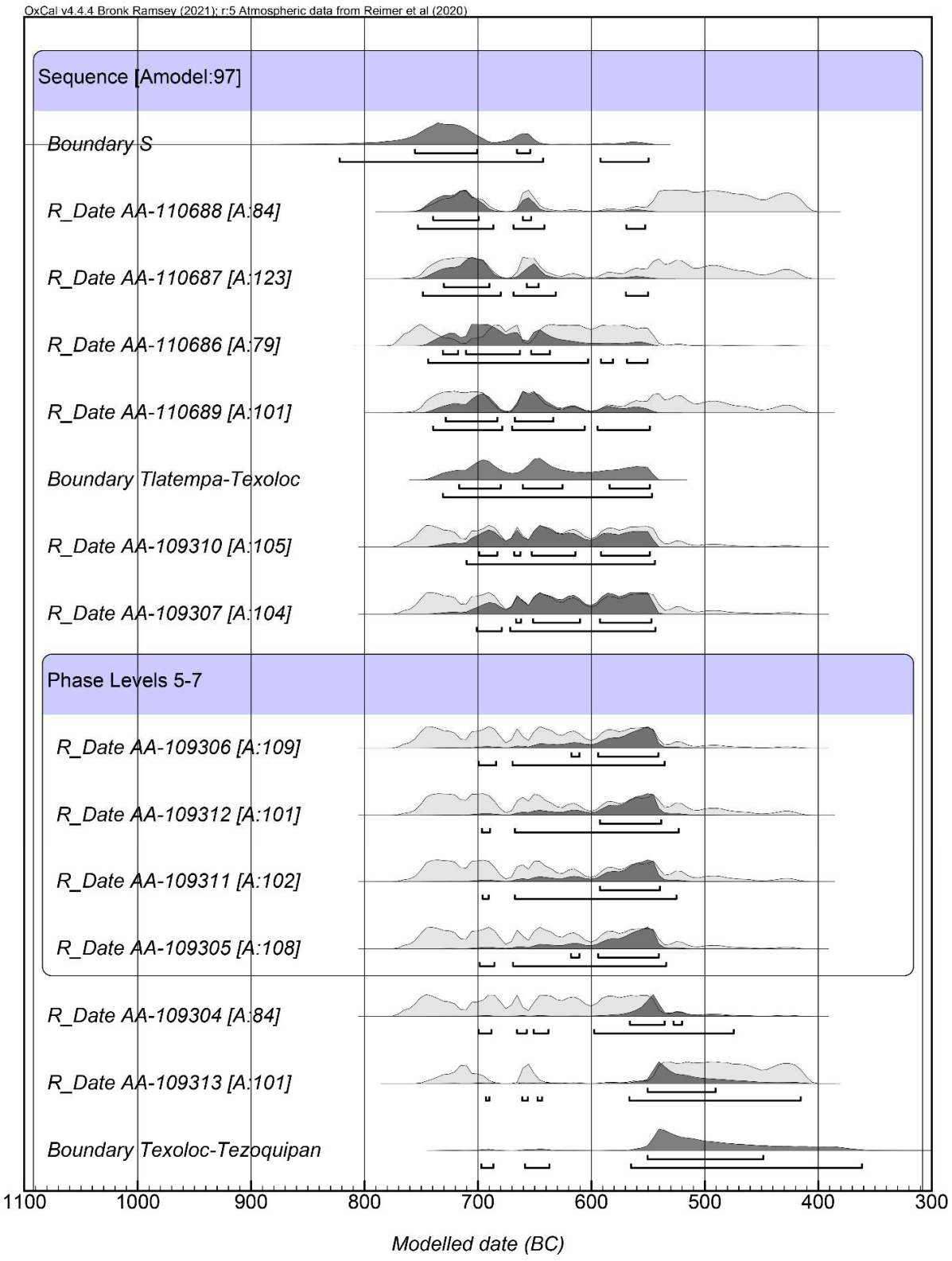

Figure S23. Bayesian Model 5 of the Middle Formative period at Tlalancaleca (Tezoquipan phase is not shown). Horizontal bars under the distributions are at 1σ and 2σ probability ranges.

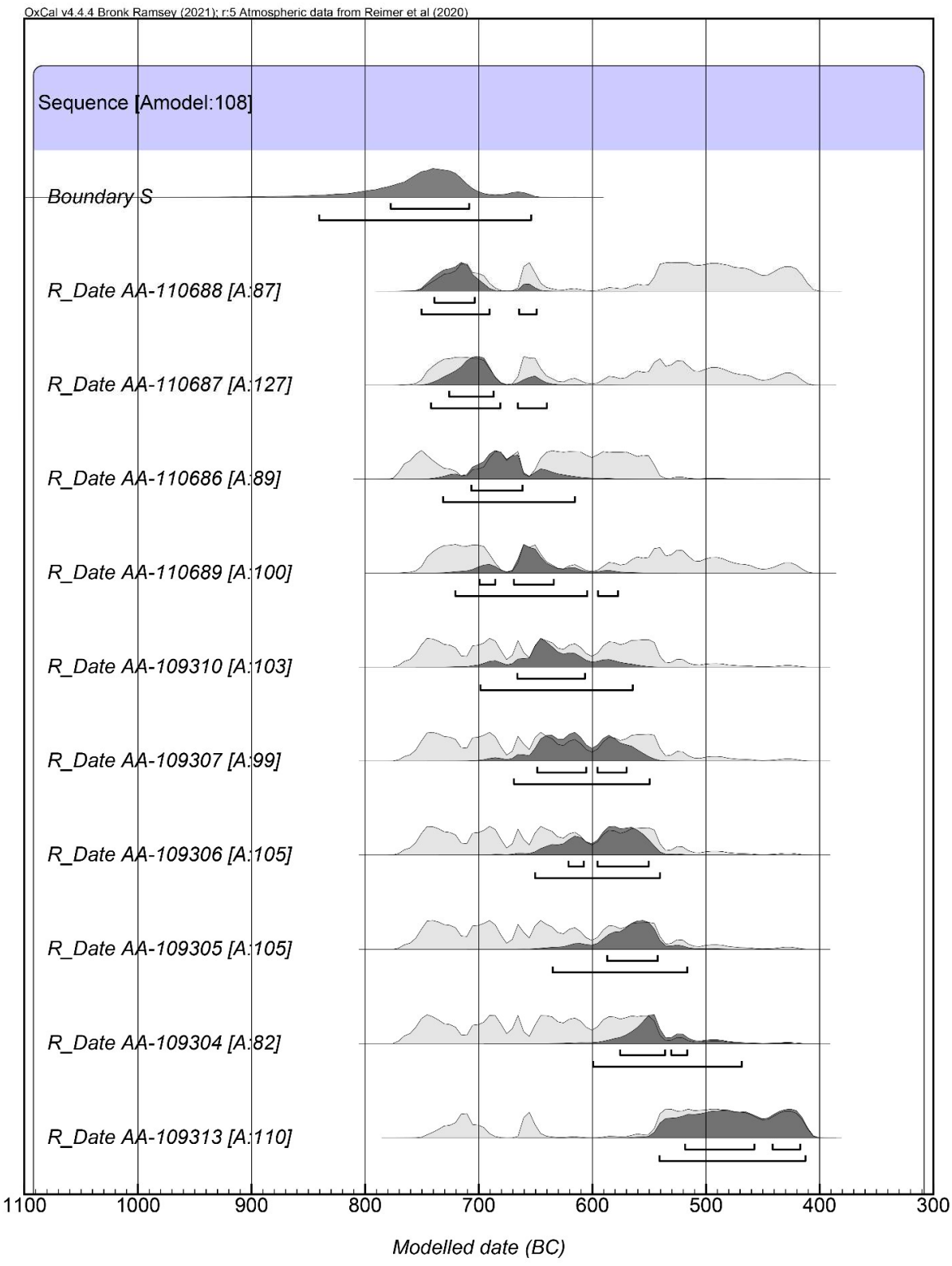

Figure S24. Bayesian Model 5NB of the Middle Formative period at Tlalancaleca (Tezoquipan phase is not shown). Horizontal bars under the distributions are at 1σ and 2σ probability ranges.

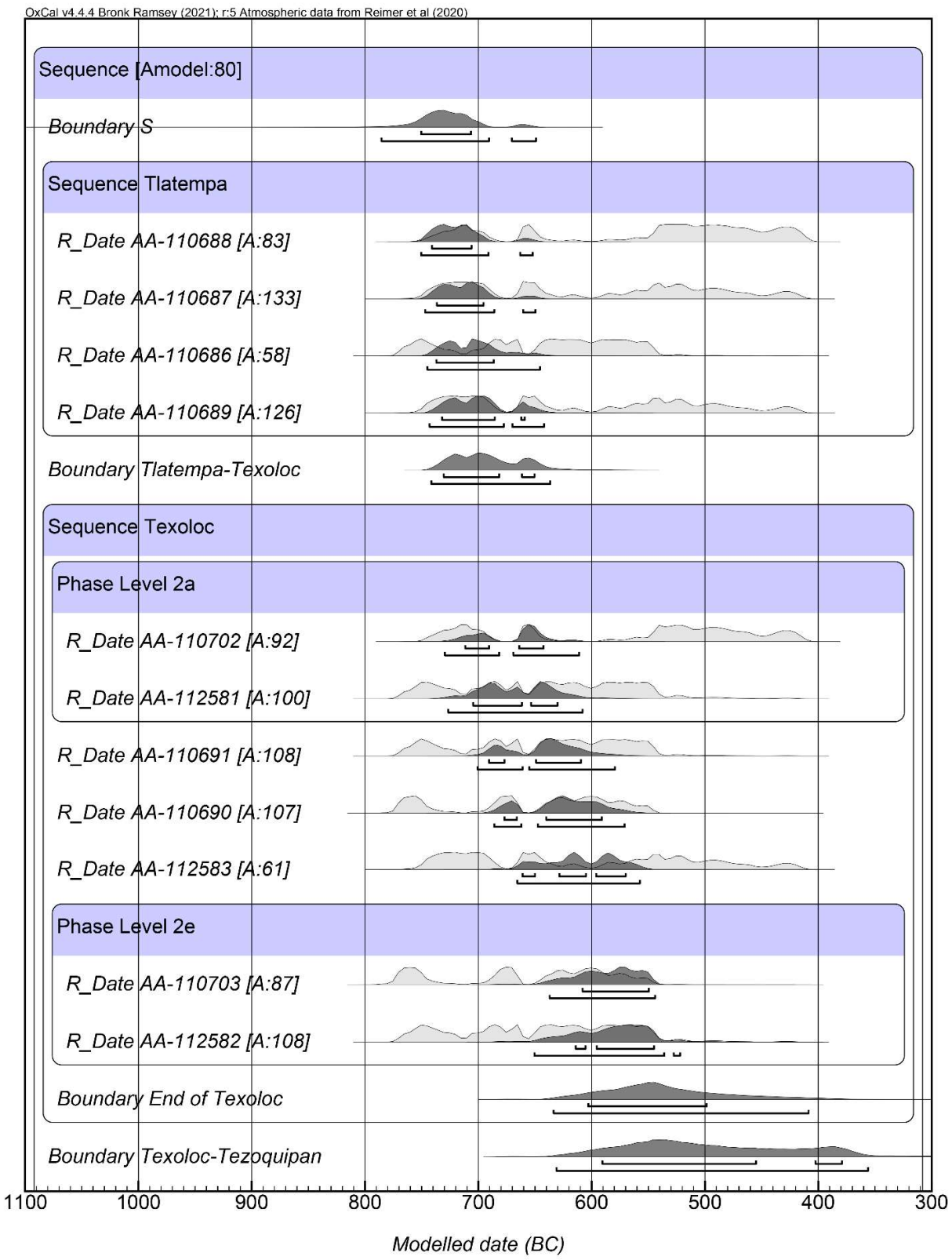

Figure S25. Bayesian Model 6 of the Middle Formative period at Tlalancaleca (Tezoquipan phase is not shown). Horizontal bars under the distributions are at 1σ and 2σ probability ranges.

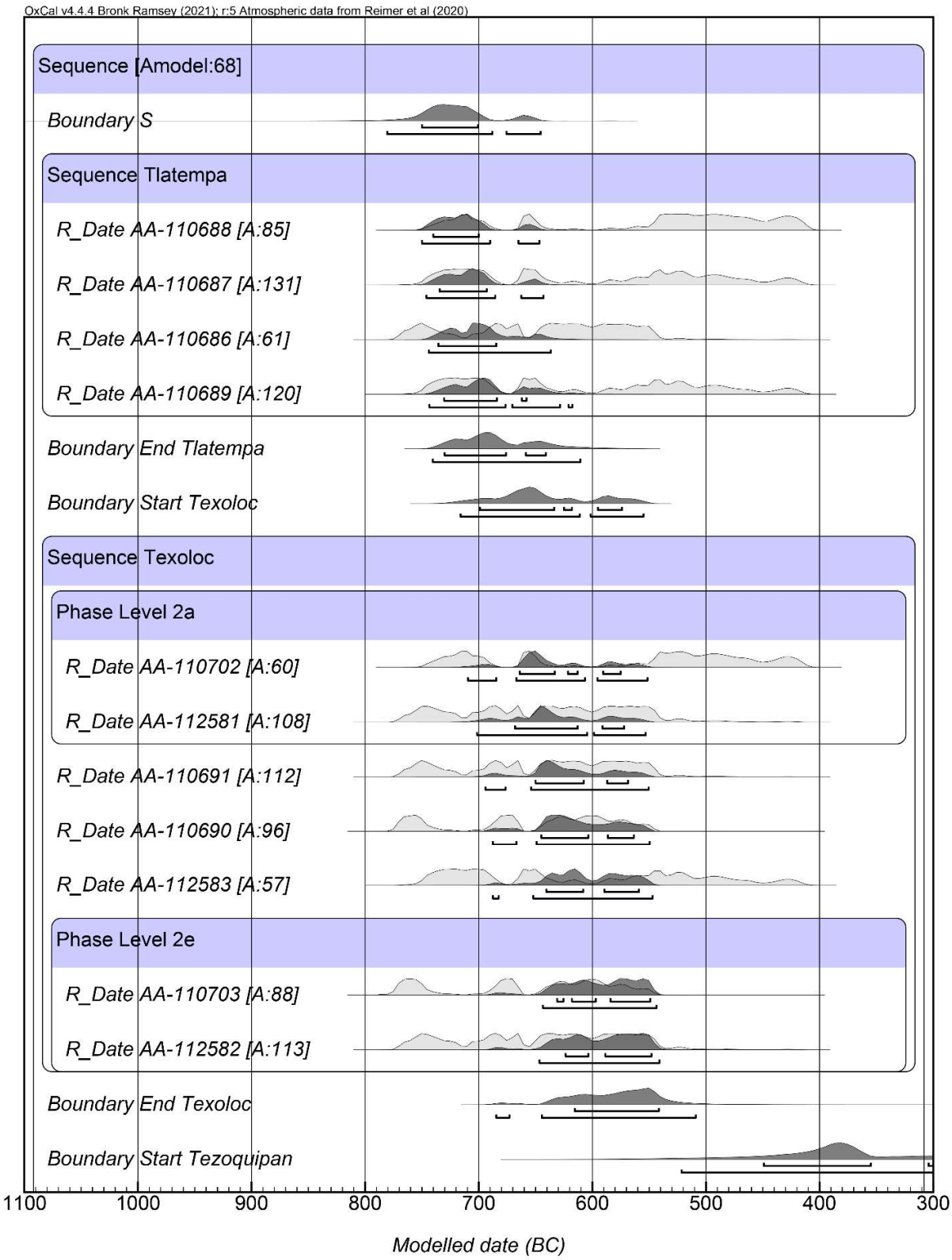

Figure S26. Bayesian Model 6S of the Middle Formative period at Tlalancaleca (Tezoquipan phase is not shown). Horizontal bars under the distributions are at 1σ and 2σ probability ranges.

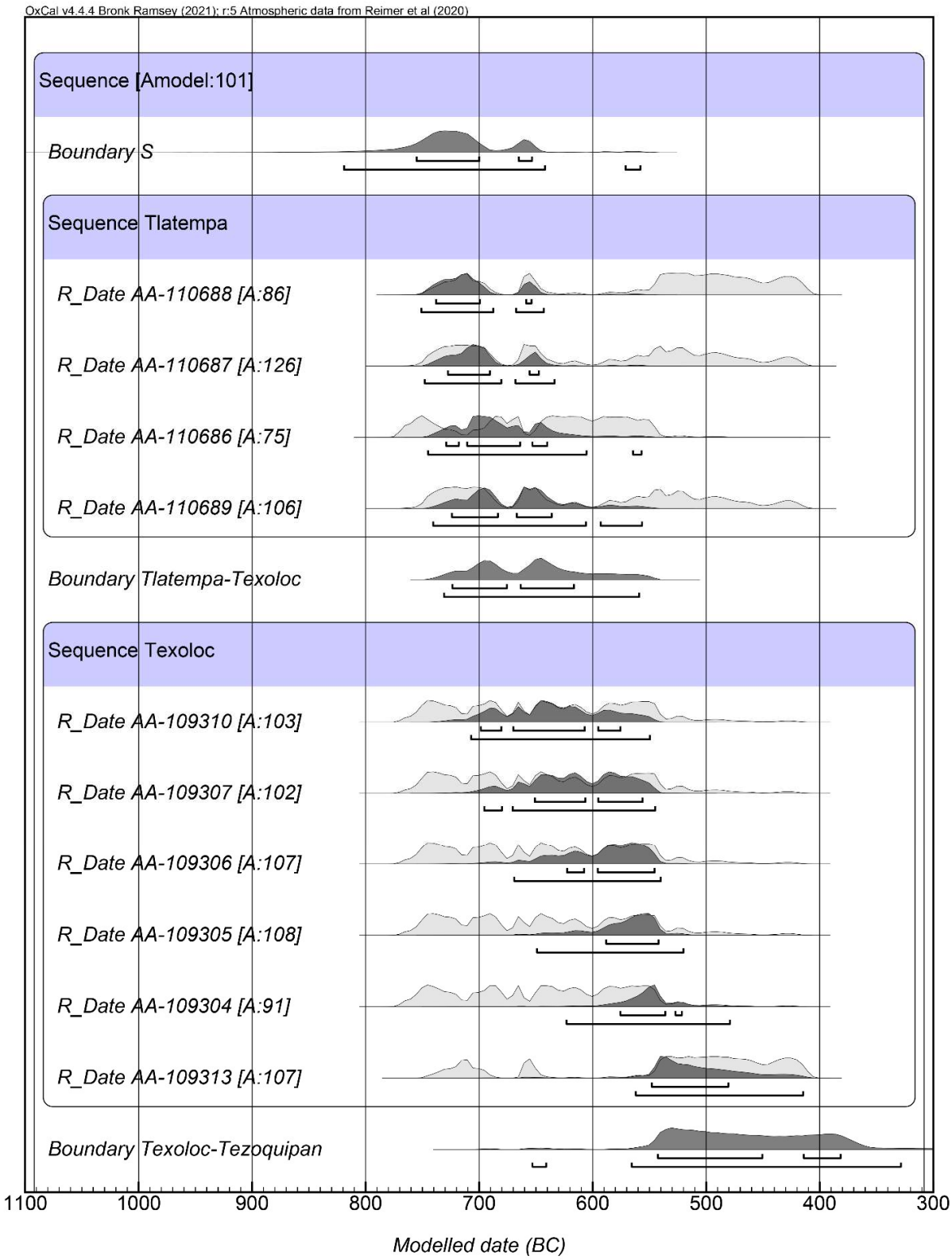

Figure S27. Bayesian Model 7 of the Middle Formative period at Tlalancaleca (Tezoquipan phase is not shown). Horizontal bars under the distributions are at 1σ and 2σ probability ranges.

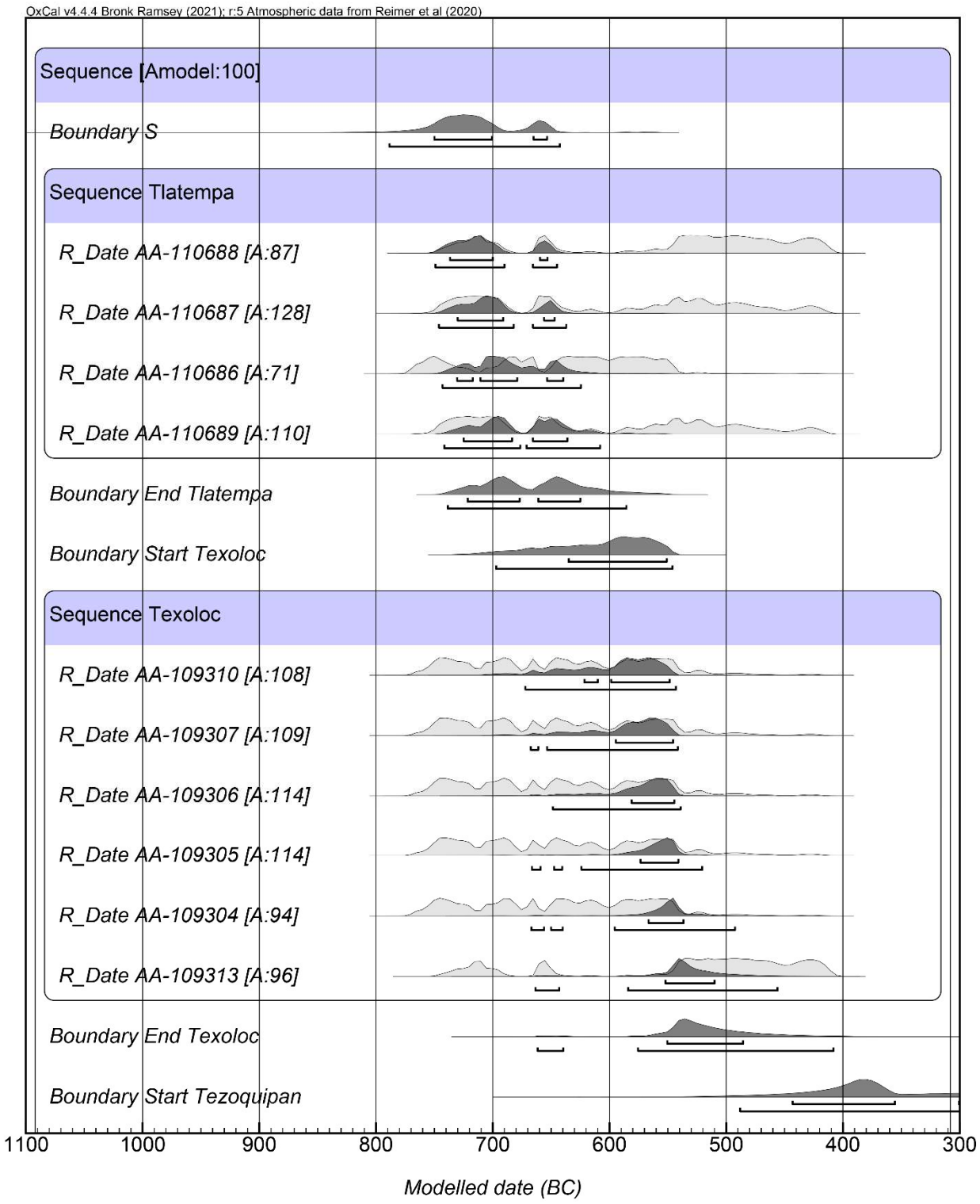

Figure S28. Bayesian Model 7S of the Middle Formative period at Tlalancaleca (Tezoquipan phase is not shown). Horizontal bars under the distributions are at 1σ and 2σ probability ranges.

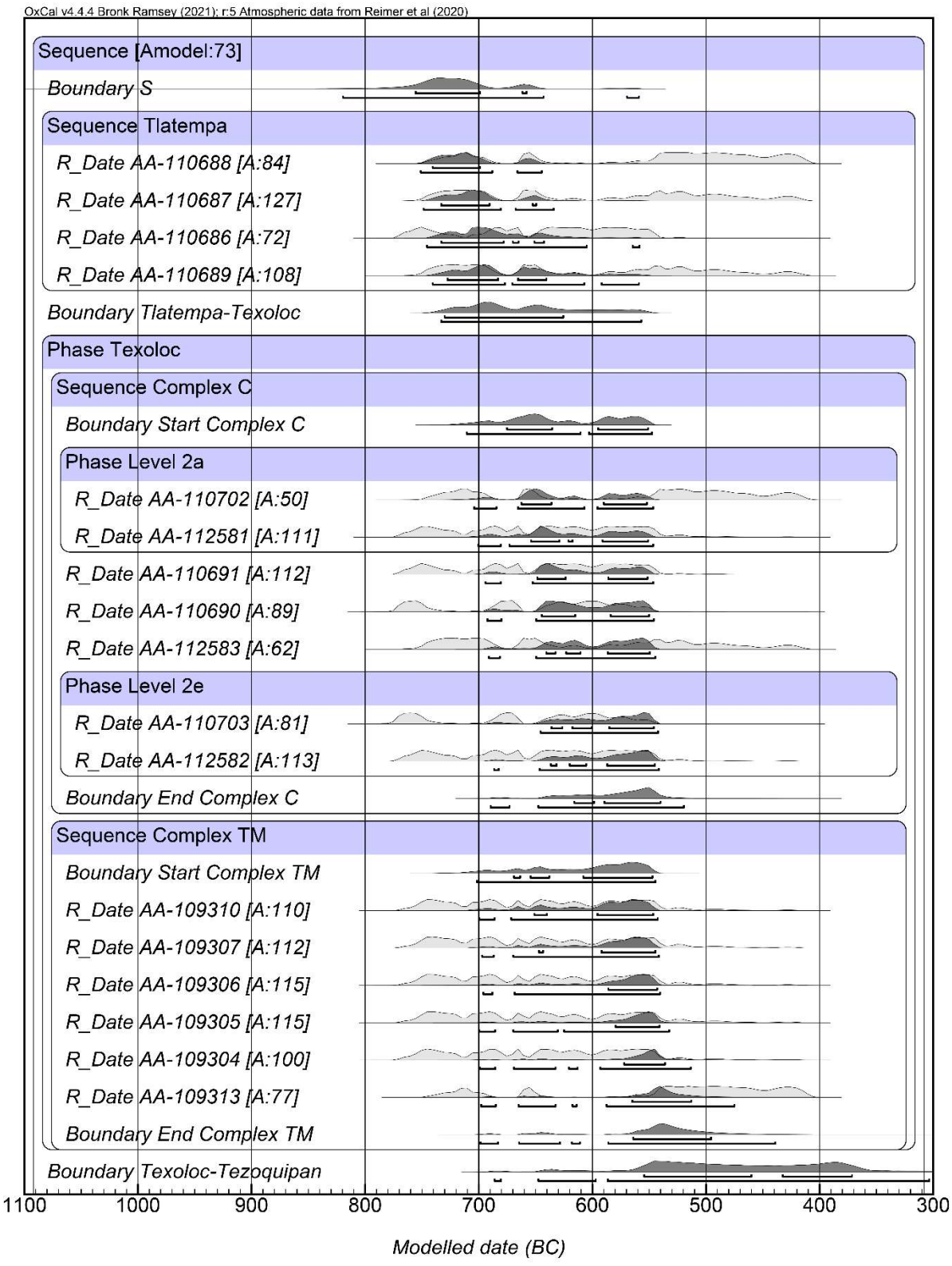

Figure S29. Bayesian Model 8 of the Middle Formative period at Tlalancaleca (Tezoquipan phase is not shown). Horizontal bars under the distributions are at 1σ and 2σ probability ranges.

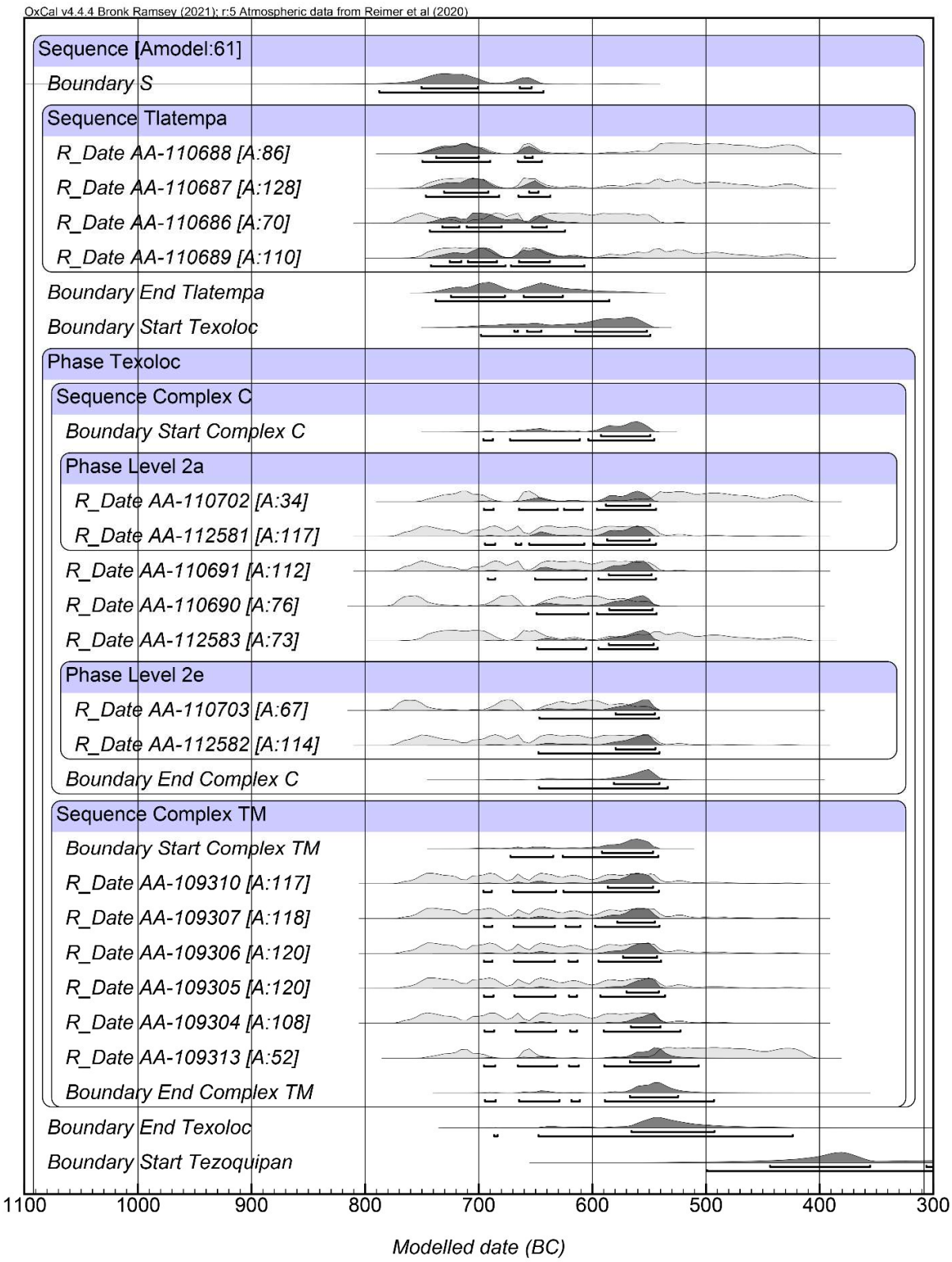

Figure S30. Bayesian Model 8S of the Middle Formative period at Tlalancaleca (Tezoquipan phase is not shown). Horizontal bars under the distributions are at 1σ and 2σ probability ranges.

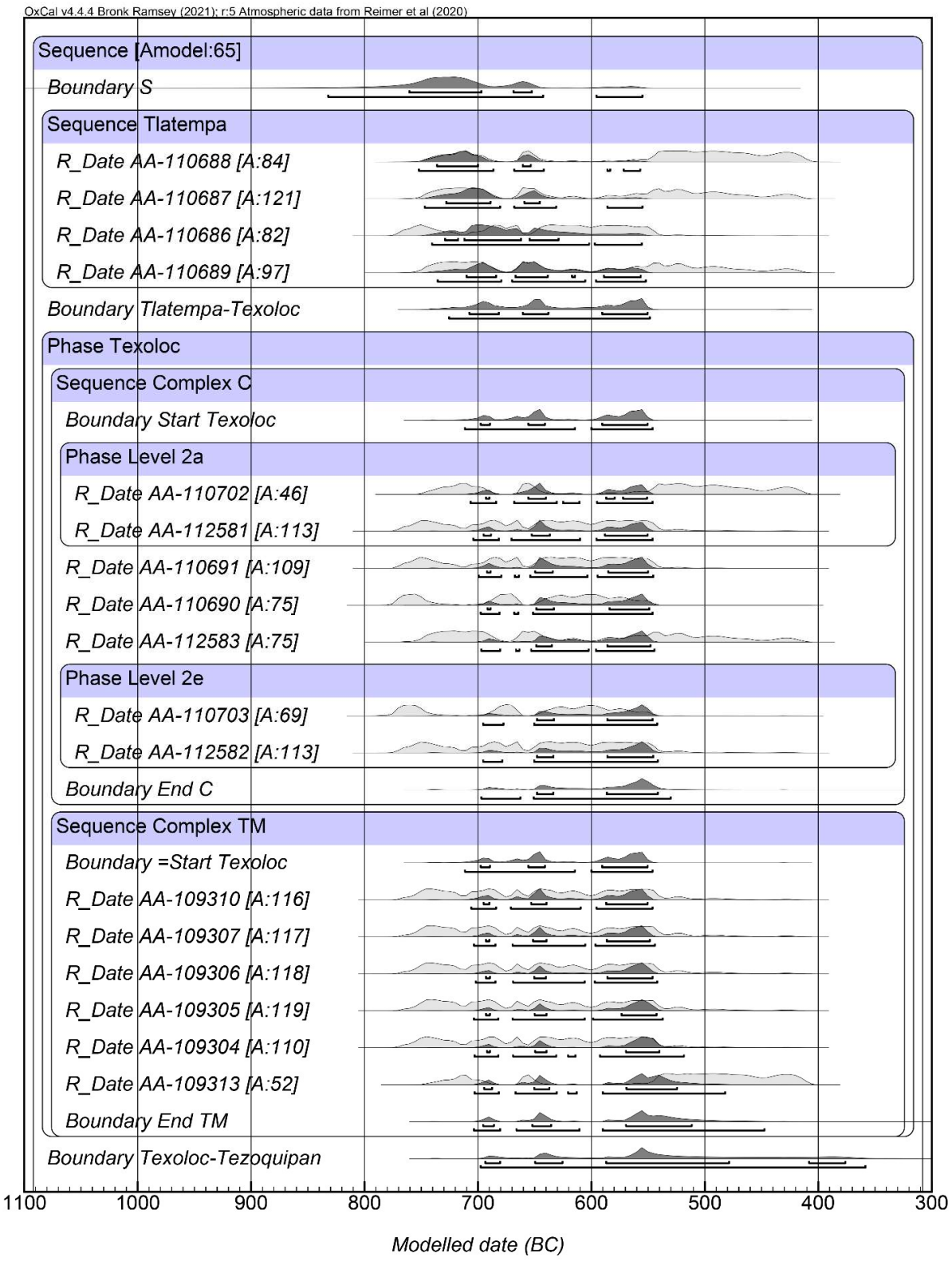

Figure S31. Bayesian Model 9 of the Middle Formative period at Tlalancaleca (Tezoquipan phase is not shown). Horizontal bars under the distributions are at 1σ and 2σ probability ranges.

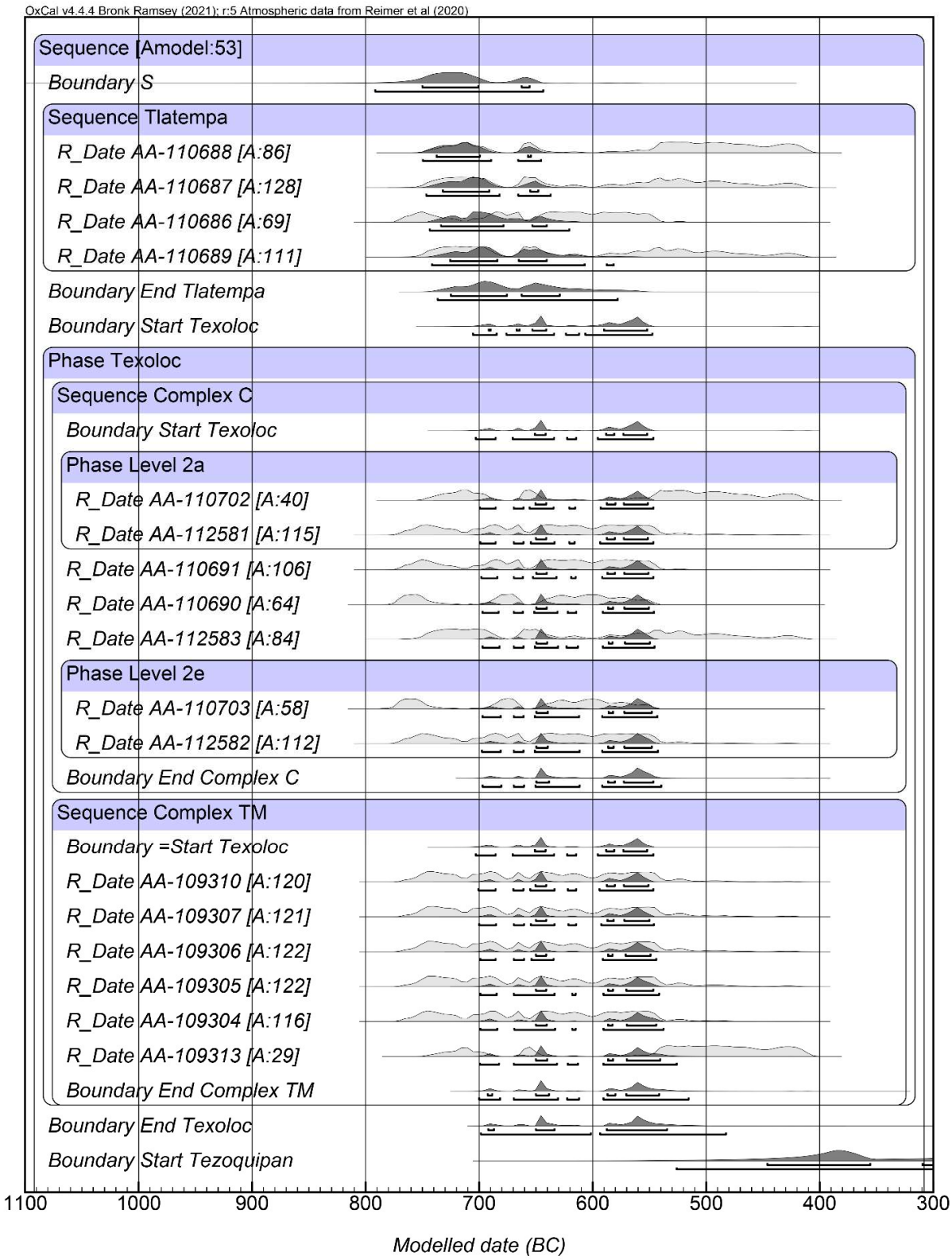

Figure S32. Bayesian Model 9S of the Middle Formative period at Tlalancaleca (Tezoquipan phase is not shown). Horizontal bars under the distributions are at 1σ and 2σ probability ranges.

Model Specifications

Charcoal Outlier Model 1

```
Plot()
{
Outlier_Model("Charcoal",T(5),U(4),"t");
Sequence()
   {
    Boundary("S");
     Phase("Texoloc")
     {
      R_Date("AA-110702",2443,19){Outlier(0.05);};
      R_Date("AA-112581",2487,22){Outlier(0.05);};
      R_Date("AA-110691",2492,19){Outlier(0.05);};
      R_Date("AA-110690",2511,19){Outlier(0.05);};
      R_Date("AA-112583",2457,21){Outlier(0.05);};
      R_Date("AA-110703",2515,20){Outlier(0.05);};
      R_Date("AA-112582",2490,22){Outlier(0.05);};
      R_Date("AA-109310", 2479, 20){Outlier(0.05);};
      R_Date("AA-109307", 2476, 20){Outlier(0.05);};
      R_Date("AA-109306", 2478, 20){Outlier(0.05);};
      R_Date("AA-109305", 2476, 20){Outlier(0.05);};
      R_Date("AA-109304", 2483, 20){Outlier(0.05);};
      R_Date("AA-109313", 2432, 20){Outlier(0.05);};
      R_Date("AA-109309", 2540, 22){Outlier(0.05);};
      R_Date("AA-109312", 2467, 21){Outlier(0.05);};
      R_Date("AA-109311", 2469, 20){Outlier(0.05);};
      R_Date("AA-109320", 2522, 21){Outlier(0.05);};
      R_Date("AA-109315", 2479, 20){Outlier(0.05);};
      R_Date("AA-110707", 2481, 20){Outlier(0.05);};
      R_Date("AA-110704",2267,19){Outlier(0.05);};
      R_Date("AA-109314",2659,20){Outlier(0.05);};
      R_Date("AA-112584",2374,21){Outlier(0.05);};
     };
    Boundary("E");
   };
   };
```

Charcoal Outlier Model 2

```
Plot()
{
Outlier_Model("Charcoal",T(5),U(4),"t");
Sequence()
   {
    Boundary("S");
    Phase("Tlatempa")
    {
     R_Date("AA-110688",2437,22){Outlier(0.05);};
     R_Date("AA-110687",2453,20){Outlier(0.05);};
     R_Date("AA-110686",2495,20){Outlier(0.05);};
     R_Date("AA-110689",2456,20){Outlier(0.05);};
     };
    Boundary("Tlatempa-Texoloc");
     Phase("Texoloc")
     {
      R_Date("AA-110702",2443,19){Outlier(0.05);};
      R_Date("AA-112581",2487,22){Outlier(0.05);};
      R_Date("AA-110691",2492,19){Outlier(0.05);};
      R_Date("AA-110690",2511,19){Outlier(0.05);};
      R_Date("AA-112583",2457,21){Outlier(0.05);};
      R_Date("AA-110703",2515,20){Outlier(0.05);};
      R_Date("AA-112582",2490,22){Outlier(0.05);};
      R_Date("AA-109310", 2479, 20){Outlier(0.05);};
      R_Date("AA-109307", 2476, 20){Outlier(0.05);};
      R_Date("AA-109306", 2478, 20){Outlier(0.05);};
      R_Date("AA-109305", 2476, 20){Outlier(0.05);};
      R_Date("AA-109304", 2483, 20){Outlier(0.05);};
      R_Date("AA-109313", 2432, 20){Outlier(0.05);};
      R_Date("AA-109309", 2540, 22){Outlier(0.05);};
      R_Date("AA-109312", 2467, 21){Outlier(0.05);};
      R_Date("AA-109311", 2469, 20){Outlier(0.05);};
      R_Date("AA-109320", 2522, 21){Outlier(0.05);};
      R_Date("AA-109315", 2479, 20){Outlier(0.05);};
      R_Date("AA-110707", 2481, 20){Outlier(0.05);};
     };
     Boundary("Texoloc-Tezoquipan");
     Phase("Tezoquipan")
     {
      R_Date("AA-105263",2168,30){Outlier(0.05);};
      R_Date("AA-110704",2267,19){Outlier(0.05);};
      R_Date("AA-110693",2249,19){Outlier(0.05);};
```

```
 };
 Boundary("E");
};
};
```

Sequence Simulation Model (6 dates with 30-year intervals)

```
Plot()
{
Sequence()
{
 Boundary("S");
 Sequence()
 {
  R_Simulate("650BC",-650,20);
  R_Simulate("620BC",-620,20);
  R_Simulate("590BC",-590,20);
  R_Simulate("560BC",-560,20);
  R_Simulate("530BC",-530,20);
  R_Simulate("500BC",-500,20);
 };
 Boundary("E");
 Span("span seq");
};
};
```

Sequence Simulation Model (11 dates with 15-year intervals)

```
Plot()
{
Sequence()
{
 Boundary("S");
 Sequence()
 {
  R_Simulate("650BC",-650,20);
  R_Simulate("635BC",-635,20);
  R_Simulate("620BC",-620,20);
  R_Simulate("605BC",-605,20);
  R_Simulate("590BC",-590,20);
  R_Simulate("575BC",-575,20);
  R_Simulate("560BC",-560,20);
  R_Simulate("545BC",-545,20);
  R_Simulate("530BC",-530,20);
  R_Simulate("515BC",-515,20);
  R_Simulate("500BC",-500,20);
 };
 Boundary("E");
 Span("span seq");
};
};
```

Sequence Simulation Model (16 dates with 10-year intervals)

```
Plot()
{
Sequence()
{
 Boundary("S");
 Sequence()
 {
  R_Simulate("650BC",-650,20);
  R_Simulate("640BC",-640,20);
  R_Simulate("630BC",-630,20);
  R_Simulate("620BC",-620,20);
  R_Simulate("610BC",-610,20);
  R_Simulate("600BC",-600,20);
  R_Simulate("590BC",-590,20);
  R_Simulate("580BC",-580,20);
  R_Simulate("570BC",-570,20);
  R_Simulate("560BC",-560,20);
  R_Simulate("550BC",-550,20);
  R_Simulate("540BC",-540,20);
  R_Simulate("530BC",-530,20);
  R_Simulate("520BC",-520,20);
  R_Simulate("510BC",-510,20);
  R_Simulate("500BC",-500,20);
 };
 Boundary("E");
 Span("span seq");
};
};
```

Phase Simulation Model (6 dates with 30-year intervals)

```
Plot()
{
Sequence()
{
 Boundary("S");
 Phase()
 {
  R_Simulate("650BC",-650,20);
  R_Simulate("620BC",-620,20);
  R_Simulate("590BC",-590,20);
  R_Simulate("560BC",-560,20);
  R_Simulate("530BC",-530,20);
  R_Simulate("500BC",-500,20);
 };
 Boundary("E");
 Span("span seq");
};
};
```

Phase Simulation Model (11 dates with 15-year intervals)

```
Plot()
{
Sequence()
{
 Boundary("S");
 Phase()
 {
  R_Simulate("650BC",-650,20);
  R_Simulate("635BC",-635,20);
  R_Simulate("620BC",-620,20);
  R_Simulate("605BC",-605,20);
  R_Simulate("590BC",-590,20);
  R_Simulate("575BC",-575,20);
  R_Simulate("560BC",-560,20);
  R_Simulate("545BC",-545,20);
  R_Simulate("530BC",-530,20);
  R_Simulate("515BC",-515,20);
  R_Simulate("500BC",-500,20);
 };
 Boundary("E");
 Span("span seq");
};
};
```

Phase Simulation Model (16 dates with 10-year intervals)

```
Plot()
{
Sequence()
{
 Boundary("S");
 Phase()
 {
  R_Simulate("650BC",-650,20);
  R_Simulate("640BC",-640,20);
  R_Simulate("630BC",-630,20);
  R_Simulate("620BC",-620,20);
  R_Simulate("610BC",-610,20);
  R_Simulate("600BC",-600,20);
  R_Simulate("590BC",-590,20);
  R_Simulate("580BC",-580,20);
  R_Simulate("570BC",-570,20);
  R_Simulate("560BC",-560,20);
  R_Simulate("550BC",-550,20);
  R_Simulate("540BC",-540,20);
  R_Simulate("530BC",-530,20);
  R_Simulate("520BC",-520,20);
  R_Simulate("510BC",-510,20);
  R_Simulate("500BC",-500,20);
 };
 Boundary("E");
 Span("span seq");
};
};
```

Model 1: Phase Method; Contiguous Model: Tlatempa (Complex C) to Texoloc (Complex C and Tres Marias)

```
Sequence()
  {
   Boundary("S");
   Phase("Tlatempa")
   {
    R_Date("AA-110688",2437,22);
    R_Date("AA-110687",2453,20);
    R_Date("AA-110686",2495,20);
    R_Date("AA-110689",2456,20);
    };
   Boundary("Tlatempa-Texoloc");
    Phase("Texoloc")
    {
     R_Date("AA-110702",2443,19);
     R_Date("AA-112581",2487,22);
     R_Date("AA-110691",2492,19);
     R_Date("AA-110690",2511,19);
     R_Date("AA-112583",2457,21);
     R_Date("AA-110703",2515,20);
     R_Date("AA-112582",2490,22);
     R_Date("AA-109310", 2479, 20);
     R_Date("AA-109307", 2476, 20);
     R_Date("AA-109306", 2478, 20);
     R_Date("AA-109305", 2476, 20);
     R_Date("AA-109304", 2483, 20);
     R_Date("AA-109313", 2432, 20);
     R_Date("AA-109309", 2540, 22);
     R_Date("AA-109312", 2467, 21);
     R_Date("AA-109311", 2469, 20);
     R_Date("AA-109320", 2522, 21);
     R_Date("AA-109315", 2479, 20);
     R_Date("AA-110707", 2481, 20);
    Interval("Duration");
    };
    Boundary("Texoloc-Tezoquipan");
    Phase("Tezoquipan")
    {
     R_Date("AA-105263",2168,30);
     R_Date("AA-110704",2267,19);
     R_Date("AA-110693",2249,19);
   };
   Boundary("E");
  };
```

Model 1S: Phase Method; Sequential Model: Tlatempa (Complex C) to Texoloc (Complex C and Tres Marias)

```
Sequence()
   {
    Boundary("Start Tlatempa");
    Phase("Tlatempa")
    {
     R_Date("AA-110688",2437,22);
     R_Date("AA-110687",2453,20);
     R_Date("AA-110686",2495,20);
     R_Date("AA-110689",2456,20);
     };
    Boundary("End Tlatempa");
    Boundary("Start Texoloc");
     Phase("Texoloc")
     {
      R_Date("AA-110702",2443,19);
      R_Date("AA-112581",2487,22);
      R_Date("AA-110691",2492,19);
      R_Date("AA-110690",2511,19);
      R_Date("AA-112583",2457,21);
      R_Date("AA-110703",2515,20);
      R_Date("AA-112582",2490,22);
      R_Date("AA-109310", 2479, 20);
      R_Date("AA-109307", 2476, 20);
      R_Date("AA-109306", 2478, 20);
      R_Date("AA-109305", 2476, 20);
      R_Date("AA-109304", 2483, 20);
      R_Date("AA-109313", 2432, 20);
      R_Date("AA-109309", 2540, 22);
      R_Date("AA-109312", 2467, 21);
      R_Date("AA-109311", 2469, 20);
      R_Date("AA-109320", 2522, 21);
      R_Date("AA-109315", 2479, 20);
      R_Date("AA-110707", 2481, 20);
     };
    Boundary("End Texoloc");
    Boundary("Start Tezoquipan");
     Phase("Tezoquipan")
     {
      R_Date("AA-105263",2168,30);
      R_Date("AA-110704",2267,19);
      R_Date("AA-110693",2249,19);
```

```
 };
 Boundary("End Tezoquipan");
};
```

Model 2: Phase Model; Contiguous Model: Tlatempa to Texoloc at the Complex C

```
Sequence()
   {
    Boundary("S");
    Phase("Tlatempa")
    {
     R_Date("AA-110688",2437,22);
     R_Date("AA-110687",2453,20);
     R_Date("AA-110686",2495,20);
     R_Date("AA-110689",2456,20);
     };
    Boundary("Tlatempa-Texoloc");
     Phase("Texoloc")
     {
      R_Date("AA-110702",2443,19);
      R_Date("AA-112581",2487,22);
      R_Date("AA-110691",2492,19);
      R_Date("AA-110690",2511,19);
      R_Date("AA-112583",2457,21);
      R_Date("AA-110703",2515,20);
      R_Date("AA-112582",2490,22);
      Interval("Duration");
     };
    Boundary("Texoloc-Tezoquipan");
     Phase("Tezoquipan")
     {
      R_Date("AA-105263",2168,30);
      R_Date("AA-110704",2267,19);
      R_Date("AA-110693",2249,19);
    };
    Boundary("E");
   };
```

Model 2S: Phase Method; Sequential Model: Tlatempa to Texoloc at the Complex C

```
Sequence()
   {
    Boundary("S");
    Phase("Tlatempa")
    {
     R_Date("AA-110688",2437,22);
     R_Date("AA-110687",2453,20);
     R_Date("AA-110686",2495,20);
     R_Date("AA-110689",2456,20);
     };
    Boundary("End Tlatempa");
    Boundary("Start Texoloc");
     Phase("Texoloc")
     {
      R_Date("AA-110702",2443,19);
      R_Date("AA-112581",2487,22);
      R_Date("AA-110691",2492,19);
      R_Date("AA-110690",2511,19);
      R_Date("AA-112583",2457,21);
      R_Date("AA-110703",2515,20);
      R_Date("AA-112582",2490,22);
     };
    Boundary("End Texoloc");
    Boundary("Start Tezoquipan");
     Phase("Tezoquipan")
     {
      R_Date("AA-105263",2168,30);
      R_Date("AA-110704",2267,19);
      R_Date("AA-110693",2249,19);
    };
    Boundary("E");
   };
```

Model 3: Phase Method; Contiguous Model: Tlatempa (Complex C) to Texoloc (Tres Marias)

```
Sequence()
   {
    Boundary("S");
    Phase("Tlatempa")
    {
     R_Date("AA-110688",2437,22);
     R_Date("AA-110687",2453,20);
     R_Date("AA-110686",2495,20);
     R_Date("AA-110689",2456,20);
     };
    Boundary("Tlatempa-Texoloc");
     Phase("Texoloc")
     {
      R_Date("AA-109310",2479,20);
      R_Date("AA-109307",2476,20);
      R_Date("AA-109306",2478,20);
      R_Date("AA-109305",2476,20);
      R_Date("AA-109304",2483,20);
      R_Date("AA-109313",2432,20);
      R_Date("AA-109309",2540,22);
      R_Date("AA-109312",2467,21);
      R_Date("AA-109311",2469,20);
      R_Date("AA-109320",2522,21);
      R_Date("AA-109315",2479,20);
      R_Date("AA-110707",2481,20);
      Interval("Duration");
     };
    Boundary("Texoloc-Tezoquipan");
     Phase("Tezoquipan")
     {
      R_Date("AA-105263",2168,30);
      R_Date("AA-110704",2267,19);
      R_Date("AA-110693",2249,19);
    };
    Boundary("E");
    };
```

Model 3S: Phase Method; Sequential Model: Tlatempa (Complex C) to Texoloc (Tres Marias)

```
Sequence()
   {
    Boundary("S");
    Phase("Tlatempa")
    {
     R_Date("AA-110688",2437,22);
     R_Date("AA-110687",2453,20);
     R_Date("AA-110686",2495,20);
     R_Date("AA-110689",2456,20);
     };
    Boundary("End Tlatempa");
    Boundary("Start Texoloc");
     Phase("Texoloc")
     {
      R_Date("AA-109310",2479,20);
      R_Date("AA-109307",2476,20);
      R_Date("AA-109306",2478,20);
      R_Date("AA-109305",2476,20);
      R_Date("AA-109304",2483,20);
      R_Date("AA-109313",2432,20);
      R_Date("AA-109309",2540,22);
      R_Date("AA-109312",2467,21);
      R_Date("AA-109311",2469,20);
      R_Date("AA-109320",2522,21);
      R_Date("AA-109315",2479,20);
      R_Date("AA-110707",2481,20);
     };
    Boundary("End Texoloc");
    Boundary("Start Tezoquipan");
     Phase("Tezoquipan")
     {
      R_Date("AA-105263",2168,30);
      R_Date("AA-110704",2267,19);
      R_Date("AA-110693",2249,19);
    };
    Boundary("E");
    };
```

Model 4: Sequence Method; Contiguous Model; Tlatempa to Texoloc at Complex C

```
Sequence()
 {
  Boundary("S");
  R_Date("AA-110688", 2437, 22);
  R_Date("AA-110687", 2453, 20);
  R_Date("AA-110686", 2495, 20);
  R_Date("AA-110689", 2456, 20);
  Boundary("Tlatempa-Texoloc");
  Phase("Level 2a")
  {
   R_Date("AA-110702", 2443, 19);
   R_Date("AA-112581", 2487, 22);
  };
  R_Date("AA-110691", 2492, 19);
  R_Date("AA-110690", 2511, 19);
  R_Date("AA-112583", 2457, 21);
  Phase("Level 2e")
  {
   R_Date("AA-110703", 2515, 20);
   R_Date("AA-112582", 2490, 22);
  };
  Boundary("Texoloc-Tezoquipan");
  Phase("Tezoquipan")
  {
   R_Date("AA-105263", 2168, 30);
   R_Date("AA-110704", 2267, 19);
   R_Date("AA-110693", 2249, 19);
  };
  Boundary("E");
 };
```

Model 4NB: Sequence Method; No boundary query; Tlatempa to Texoloc at Complex C

```
Sequence()
   {
    Boundary("S");
     R_Date("AA-110688",2437,22);
     R_Date("AA-110687",2453,20);
     R_Date("AA-110686",2495,20);
     R_Date("AA-110689",2456,20);
     Phase("Level 2a")
     {
      R_Date("AA-110702",2443,19);
      R_Date("AA-112581",2487,22);
      };
      R_Date("AA-110691",2492,19);
      R_Date("AA-110690",2511,19);
      R_Date("AA-112583",2457,21);
     Phase("Level 2e")
     {
      R_Date("AA-110703",2515,20);
      R_Date("AA-112582",2490,22);
     };
     Phase("Tezoquipan")
     {
      R_Date("AA-105263",2168,30);
      R_Date("AA-110704",2267,19);
      R_Date("AA-110693",2249,19);
    };
    Boundary("E");
   };
```

Model 5: Sequence Method; Contiguous Model; Tlatempa (Complex C) to Texoloc (Tres Marias)

```
Sequence()
   {
    Boundary("S");
     R_Date("AA-110688",2437,22);
     R_Date("AA-110687",2453,20);
     R_Date("AA-110686",2495,20);
     R_Date("AA-110689",2456,20);
     Boundary("Tlatempa-Texoloc");
      R_Date("AA-109310", 2479, 20);
      R_Date("AA-109307", 2476, 20);
     Phase("Levels 5-7")
     {
      R_Date("AA-109306", 2478, 20);
      R_Date("AA-109312", 2467, 21);
      R_Date("AA-109311", 2469, 20);
      R_Date("AA-109305", 2476, 20);
      };
      R_Date("AA-109304", 2483, 20);
      R_Date("AA-109313", 2432, 20);
     Boundary("Texoloc-Tezoquipan");
     Phase("Tezoquipan")
     {
      R_Date("AA-105263",2168,30);
      R_Date("AA-110704",2267,19);
      R_Date("AA-110693",2249,19);
     };
     Boundary("E");
    };
```

Model 5NB: Sequence Method; No boundary query; Tlatempa (Complex C) to Texoloc (Tres Marias)

```
Sequence()
   {
    Boundary("S");
     R_Date("AA-110688",2437,22);
     R_Date("AA-110687",2453,20);
     R_Date("AA-110686",2495,20);
     R_Date("AA-110689",2456,20);
      R_Date("AA-109310", 2479, 20);
      R_Date("AA-109307", 2476, 20);
      R_Date("AA-109306", 2478, 20);
      R_Date("AA-109305", 2476, 20);
      R_Date("AA-109304", 2483, 20);
      R_Date("AA-109313", 2432, 20);
     Phase("Tezoquipan")
     {
      R_Date("AA-105263",2168,30);
      R_Date("AA-110704",2267,19);
      R_Date("AA-110693",2249,19);
    };
    Boundary("E");
   };
```

Model 6: Phase/Sequence Method; Contiguous Model; Tlatempa to Texoloc at Complex C

```
Sequence()
  {
   Boundary("S");
    Sequence ("Tlatempa")
    {
      R_Date("AA-110688",2437,22);
      R_Date("AA-110687",2453,20);
      R_Date("AA-110686",2495,20);
      R_Date("AA-110689",2456,20);
     };
    Boundary("Tlatempa-Texoloc");
    Sequence("Texoloc")
    {
      Phase("Level 2a")
      {
      R_Date("AA-110702",2443,19);
      R_Date("AA-112581",2487,22);
      };
      R_Date("AA-110691",2492,19);
      R_Date("AA-110690",2511,19);
      R_Date("AA-112583",2457,21);
      Phase("Level 2e")
       {
       R_Date("AA-110703",2515,20);
       R_Date("AA-112582",2490,22);
       };
       };
      Boundary("Texoloc-Tezoquipan");
    Phase("Tezoquipan")
    {
     R_Date("AA-105263",2168,30);
     R_Date("AA-110704",2267,19);
     R_Date("AA-110693",2249,19);
   };
   Boundary("E");
  };
```

Model 6S: Phase/Sequence Method; Sequential Model; Tlatempa to Texoloc at Complex C

```
Sequence()
  {
   Boundary("S");
    Sequence ("Tlatempa")
    {
      R_Date("AA-110688",2437,22);
      R_Date("AA-110687",2453,20);
      R_Date("AA-110686",2495,20);
      R_Date("AA-110689",2456,20);
     };
    Boundary("End Tlatempa ");
    Boundary("Start Texoloc");
    Sequence("Texoloc")
    {
      Phase("Level 2a")
      {
      R_Date("AA-110702",2443,19);
      R_Date("AA-112581",2487,22);
      };
      R_Date("AA-110691",2492,19);
      R_Date("AA-110690",2511,19);
      R_Date("AA-112583",2457,21);
      Phase("Level 2e")
       {
       R_Date("AA-110703",2515,20);
       R_Date("AA-112582",2490,22);
       };
      };
   Boundary("End of Texoloc");
    Boundary("Start Tezoquipan");
    Phase("Tezoquipan")
    {
     R_Date("AA-105263",2168,30);
     R_Date("AA-110704",2267,19);
     R_Date("AA-110693",2249,19);
   };
   Boundary("E");
  };
```

Model 7: Phase/Sequence Model; Contiguous Model; Tlatempa (Complex C) to Texoloc (Tres Marias)

```
Sequence()
   {
    Boundary("S");
    Sequence("Tlatempa")
    {
     R_Date("AA-110688",2437,22);
     R_Date("AA-110687",2453,20);
     R_Date("AA-110686",2495,20);
     R_Date("AA-110689",2456,20);
     };
     Boundary("Tlatempa-Texoloc");
     Sequence("Texoloc")
     {
     R_Date("AA-109310", 2479, 20);
     R_Date("AA-109307", 2476, 20);
     R_Date("AA-109306", 2478, 20);
     R_Date("AA-109305", 2476, 20);
     R_Date("AA-109304", 2483, 20);
     R_Date("AA-109313", 2432, 20);
     Interval("Duration of Texoloc");
     };
    Boundary("Texoloc-Tezoquipan");
    Phase("Tezoquipan")
     {
      R_Date("AA-105263",2168,30);
      R_Date("AA-110704",2267,19);
      R_Date("AA-110693",2249,19);
    };
    Boundary("E");
   };
```

Model 7S: Phase/Sequence Model; Sequential Model; Tlatempa (Complex C) to Texoloc (Tres Marias)

```
Sequence ()
   {
    Boundary("S");
    Sequence("Tlatempa")
    {
     R_Date("AA-110688",2437,22);
     R_Date("AA-110687",2453,20);
     R_Date("AA-110686",2495,20);
     R_Date("AA-110689",2456,20);
     };
     Boundary("End Tlatempa");
     Boundary("Start Texoloc");
     Sequence("Texoloc")
     {
     R_Date("AA-109310", 2479, 20);
     R_Date("AA-109307", 2476, 20);
     R_Date("AA-109306", 2478, 20);
     R_Date("AA-109305", 2476, 20);
     R_Date("AA-109304", 2483, 20);
     R_Date("AA-109313", 2432, 20);
     };
    Boundary("End Texoloc");
    Boundary("Start Tezoquipan");
    Phase("Tezoquipan")
     {
      R_Date("AA-105263",2168,30);
      R_Date("AA-110704",2267,19);
      R_Date("AA-110693",2249,19);
    };
    Boundary("E");
   };
```

Model 8: Overlapping Sequence Method; Contiguous Model; Tlatempa (Complex C) to Texoloc (Complex C and Tres Marias)

```
Sequence()
   {
    Boundary("S");
     Sequence ("Tlatempa")
     {
       R_Date("AA-110688",2437,22);
       R_Date("AA-110687",2453,20);
       R_Date("AA-110686",2495,20);
       R_Date("AA-110689",2456,20);
      };
     Boundary("Tlatempa-Texoloc");
     Phase("Texoloc")
     {
     Sequence("Complex C")
     {
      Boundary("Start Complex C");
       Phase("Level 2a")
       {
       R_Date("AA-110702",2443,19);
       R_Date("AA-112581",2487,22);
       };
       R_Date("AA-110691",2492,19);
       R_Date("AA-110690",2511,19);
       R_Date("AA-112583",2457,21);
       Phase("Level 2e")
        {
        R_Date("AA-110703",2515,20);
        R_Date("AA-112582",2490,22);
        };
       Boundary("End Complex C");
      };
Sequence("Complex TM")
     {
    Boundary("Start Complex TM");
     R_Date("AA-109310", 2479, 20);
     R_Date("AA-109307", 2476, 20);
     R_Date("AA-109306", 2478, 20);
     R_Date("AA-109305", 2476, 20);
     R_Date("AA-109304", 2483, 20);
     R_Date("AA-109313", 2432, 20);
     Boundary("End Complex TM");
     };
   };
     Boundary("Texoloc-Tezoquipan");
     Phase("Tezoquipan")
```

```
 {
  R_Date("AA-105263",2168,30);
  R_Date("AA-110704",2267,19);
  R_Date("AA-110693",2249,19);
 };
 Boundary("E");
};
```

Model 8S: Overlapping Sequence Method; Sequential Model; Tlatempa (Complex C) to Texoloc (Complex C and Tres Marias)

```
Sequence()
   {
    Boundary("S");
     Sequence ("Tlatempa")
     {
       R_Date("AA-110688",2437,22);
       R_Date("AA-110687",2453,20);
       R_Date("AA-110686",2495,20);
       R_Date("AA-110689",2456,20);
      };
     Boundary("End Tlatempa");
     Boundary("Start Texoloc");
     Phase("Texoloc")
     {
     Sequence("Complex C")
     {
      Boundary("Start Complex C");
       Phase("Level 2a")
       {
       R_Date("AA-110702",2443,19);
       R_Date("AA-112581",2487,22);
       };
       R_Date("AA-110691",2492,19);
       R_Date("AA-110690",2511,19);
       R_Date("AA-112583",2457,21);
       Phase("Level 2e")
        {
        R_Date("AA-110703",2515,20);
        R_Date("AA-112582",2490,22);
        };
       Boundary("End Complex C");
      };
Sequence("Complex TM")
     {
    Boundary("Start Complex TM");
     R_Date("AA-109310", 2479, 20);
     R_Date("AA-109307", 2476, 20);
     R_Date("AA-109306", 2478, 20);
     R_Date("AA-109305", 2476, 20);
     R_Date("AA-109304", 2483, 20);
     R_Date("AA-109313", 2432, 20);
     Boundary("End Complex TM");
     };
   };
```

```
 Boundary("End Texoloc");
 Boundary("Start Tezoquipan");
 Phase("Tezoquipan")
 {
  R_Date("AA-105263",2168,30);
  R_Date("AA-110704",2267,19);
  R_Date("AA-110693",2249,19);
 };
 Boundary("E");
};
```

Model 9: Cross Referencing Method; Contiguous Model; Tlatempa (Complex C) to Texoloc (Complex C and Tres Marias)

```
Sequence()
   {
    Boundary("S");
     Sequence ("Tlatempa")
     {
       R_Date("AA-110688",2437,22);
       R_Date("AA-110687",2453,20);
       R_Date("AA-110686",2495,20);
       R_Date("AA-110689",2456,20);
      };
     Boundary("Tlatempa-Texoloc");
     Phase("Texoloc")
     {
     Sequence("Complex C")
     {
      // first instance of the parameter "Start Texoloc"
      Boundary("Start Texoloc");
       Phase("Level 2a")
       {
       R_Date("AA-110702",2443,19);
       R_Date("AA-112581",2487,22);
       };
       R_Date("AA-110691",2492,19);
       R_Date("AA-110690",2511,19);
       R_Date("AA-112583",2457,21);
       Phase("Level 2e")
        {
        R_Date("AA-110703",2515,20);
        R_Date("AA-112582",2490,22);
        };
       Boundary("End C");
      };
Sequence("Complex TM")
    {
    // cross reference to the parameter "Start Texoloc"
    Boundary("=Start Texoloc");
     R_Date("AA-109310", 2479, 20);
     R_Date("AA-109307", 2476, 20);
     R_Date("AA-109306", 2478, 20);
     R_Date("AA-109305", 2476, 20);
     R_Date("AA-109304", 2483, 20);
     R_Date("AA-109313", 2432, 20);
     Boundary("End TM");
     };
   };
```

```
 Boundary("Texoloc-Tezoquipan");
 Phase("Tezoquipan")
 {
  R_Date("AA-105263",2168,30);
  R_Date("AA-110704",2267,19);
  R_Date("AA-110693",2249,19);
 };
 Boundary("E");
};
```

Model 9S: Cross Referencing Method; Contiguous Model; Tlatempa (Complex C) to Texoloc (Complex C and Tres Marias)

```
Sequence()
   {
    Boundary("S");
     Sequence ("Tlatempa")
     {
       R_Date("AA-110688",2437,22);
       R_Date("AA-110687",2453,20);
       R_Date("AA-110686",2495,20);
       R_Date("AA-110689",2456,20);
      };
     Boundary("End Tlatempa");
     Boundary("Start Texoloc");
     Phase("Texoloc")
     {
     Sequence("Complex C")
     {
       // first instance of the parameter "Start Texoloc"
       Boundary("Start Texoloc");
        Phase("Level 2a")
        {
       R_Date("AA-110702",2443,19);
       R_Date("AA-112581",2487,22);
       };
       R_Date("AA-110691",2492,19);
       R_Date("AA-110690",2511,19);
       R_Date("AA-112583",2457,21);
       Phase("Level 2e")
        {
        R_Date("AA-110703",2515,20);
        R_Date("AA-112582",2490,22);
        };
       Boundary("End Complex C");
      };
Sequence("Complex TM")
     {
    // cross reference to the parameter "Start Texoloc"
    Boundary("=Start Texoloc");
     R_Date("AA-109310", 2479, 20);
     R_Date("AA-109307", 2476, 20);
     R_Date("AA-109306", 2478, 20);
     R_Date("AA-109305", 2476, 20);
     R_Date("AA-109304", 2483, 20);
     R_Date("AA-109313", 2432, 20);
     Boundary("End Complex TM");
     };
```

```
};
 Boundary("End Texoloc");
 Boundary("Start Tezoquipan");
 Phase("Tezoquipan")
 {
  R_Date("AA-105263",2168,30);
  R_Date("AA-110704",2267,19);
  R_Date("AA-110693",2249,19);
 };
 Boundary("E");
};
```